Cerebral Cortex July 2011;21:1674-1694
doi:10.1093/cercor/bhq238
Advance Access publication December 2, 2010

A Role for Intermediate Radial Glia in the Tangential Expansion of the Mammalian Cerebral Cortex

Isabel Reillo[1], Camino de Juan Romero[1], Miguel Ángel García-Cabezas[2] and Víctor Borrell[1]

[1]Developmental Neurobiology Unit, Instituto de Neurociencias, Consejo Superior de Investigaciones Científicas-Universidad Miguel Hernández, 03550 Sant Joan d'Alacant, Spain and [2]Department of Pathology, Hospital Universitario La Paz, 28029 Madrid, Spain

Address correspondence to Víctor Borrell, Instituto de Neurociencias, Consejo Superior de Investigaciones Científicas-Universidad Miguel Hernández, Avenida Ramón y Cajal s/n, 03550 Sant Joan d'Alacant, Spain. Email: vborrell@umh.es.

The cerebral cortex of large mammals undergoes massive surface area expansion and folding during development. Specific mechanisms to orchestrate the growth of the cortex in surface area rather than in thickness are likely to exist, but they have not been identified. Analyzing multiple species, we have identified a specialized type of progenitor cell that is exclusive to mammals with a folded cerebral cortex, which we named intermediate radial glia cell (IRGC). IRGCs express Pax6 but not Tbr2, have a radial fiber contacting the pial surface but not the ventricular surface, and are found in both the inner subventricular zone and outer subventricular zone (OSVZ). We find that IRGCs are massively generated in the OSVZ, thus augmenting the numbers of radial fibers. Fanning out of this expanding radial fiber scaffold promotes the tangential dispersion of radially migrating neurons, allowing for the growth in surface area of the cortical sheet. Accordingly, the tangential expansion of particular cortical regions was preceded by high proliferation in the underlying OSVZ, whereas the experimental reduction of IRGCs impaired the tangential dispersion of neurons and resulted in a smaller cortical surface. Thus, the generation of IRGCs plays a key role in the tangential expansion of the mammalian cerebral cortex.

Keywords: enucleation, gyrus, neurogenesis, OSVZ, Pax6

Introduction

An extraordinary expansion in brain size during mammalian evolution is thought to underlie the growth of intellectual capacity. Most of this expansion is due to a massive increase in surface area of the multilayered sheet of neurons forming the cerebral cortex (Finlay and Darlington 1995). Such expansion in cortical surface area, which is about 1000 times larger in humans than in mice, is not accompanied by a proportionate difference in thickness (only ~2 times thicker in humans than mice) but rather comes together with the appearance of convolutions of the cortical sheet (gyrencephaly), with folds and fissures known as gyri and sulci (Welker 1990; Rakic 1995a). Notably, human mutations causing a loss of cortical convolutions (lissencephaly) result in severe reductions of intellectual performance (Ross and Walsh 2001; Sheen and Walsh 2003).

The cerebral cortex is functionally organized in radial columns of interconnected neurons, and the evolutionary expansion of the cortical surface area is thought to have involved the generation of additional columns by cortical progenitors (Rakic 1988, 1995a). Remarkably, the sheet of cells containing the majority of cortical progenitors, the ventricular zone (VZ) (Boulder Committee 1970; Bayer and Altman 1991), displays no convolutions, regardless of whether progenitors are to generate a smooth cortex (i.e., in mice) or a profoundly gyrated cortex (i.e., in humans) (Smart and McSherry 1986b; Welker 1990; Armstrong et al. 1995; Rakic 1995a; Smart et al. 2002). Recent studies demonstrate that the late-appearing cortical subventricular zone (SVZ) houses a population of secondary progenitors (Noctor et al. 2004; Lukaszewicz et al. 2005). In primates, the SVZ is much thicker than in rodents and is subdivided into inner subventricular zone (ISVZ) and outer subventricular zone (OSVZ) (Smart et al. 2002; Zecevic et al. 2005; Martinez-Cerdeno et al. 2006). The human OSVZ has been intensely studied both in vivo and in vitro, and shown to be a very complex layer, containing not only a highly heterogeneous population of cortical progenitors but also radially and tangentially migrating neurons, axonal fibers, and displaced radial glia cells (Sidman and Rakic 1973; Letinic et al. 2002; deAzevedo et al. 2003; Zecevic 2004; Zecevic et al. 2005; Howard et al. 2006; Mo et al. 2007; Mo and Zecevic 2008, 2009; Hansen et al. 2010). Because the OSVZ exists in primates but not in rodents and because it has such a complex cellular composition, it has been proposed that the OSVZ may be a primate unique feature playing a central role in the development of the singularly complex primate cerebral cortex, including its tangential expansion and folding (Rakic 1995a, 2009; Kriegstein et al. 2006; Dehay and Kennedy 2007; Bystron et al. 2008 and references therein). However, the histogenetic mechanisms governing the tangential expansion and folding of the cerebral cortex in large mammals (including primates and nonprimates) are still unknown, and their identification is essential to understand the role of genes critically involved in this process.

Here we have studied cellular mechanisms involved in the tangential expansion of the cerebral cortex in higher mammals. We begin by showing that the histological subdivision of the SVZ into ISVZ and OSVZ is a feature common to gyrencephalic species, not unique to primates, and confirm that lissencephalic species do not exhibit OSVZ. We also show that nonprimate OSVZ progenitors are highly heterogeneous and include a transient form of radial glia, which we have named intermediate radial glia cell (IRGC). IRGCs are characterized by having a radial fiber extended to the pial surface but without a process contacting the ventricular surface, by expressing Pax6 but not Tbr2, and by being self-amplifying progenitors. Previous studies have described cells with similar characteristics in ferret and in the human OSVZ (named OSVZ radial glia [oRG; Fietz et al. 2010; Hansen et al. 2010]), whereas here we find that IRGCs exist in both the OSVZ and the ISVZ. Further analyses indicate that the addition of radial fibers by new IRGCs contributes to a progressive divergence of the radial fiber scaffold. This process results in the fanned

© The Author 2010. Published by Oxford University Press. All rights reserved.
For permissions, please e-mail: journals.permissions@oup.com

Downloaded from https://academic.oup.com/cercor/article/21/7/1674/339599 by guest on 23 April 2024

spreading of radially migrating neurons over a wide range of trajectories and directly determines their tangential dispersion along the cortical surface. Experiments of binocular enucleation in ferret demonstrate that a selective decrease in OSVZ proliferation reduces the tangential dispersion of cortical neurons and, in turn, the surface area of the visual cerebral cortex. These findings provide experimental evidence that OSVZ proliferation and IRGC production are key events for the tangential expansion of the cerebral cortex in gyrencephalic mammals.

Materials and Methods

Animals

Wild-type mice were maintained in an ICR background, and guinea pigs were maintained in an albino background. The day of vaginal plug was considered as embryonic day (E) 0.5. Pigmented ferrets (*Mustela putorius furo*) were obtained from Marshall Farms and kept on a 12:12 h light:dark cycle. Domestic cat (*Felix domestica*) embryos were obtained from a breeding colony. Mice, guinea pigs, ferrets, and cats were kept at the Animal Facilities of the Universidad Miguel Hernández, where animals were treated according with Spanish and EU regulations and experimental protocols were approved by the Universidad Miguel Hernández IACUC. Part of the ferret surgeries and sample collections were performed under the auspices of Edward M. Callaway at The Salk Institute for Biological Studies, La Jolla, CA, where animals were treated in accordance with institutional guidelines and experimental protocols approved by the Salk Institute IACUC. Live sheep embryos were obtained from the slaughter house MURGACA by permission and under supervision of the veterinary in chief. The embryonic age of collected embryos was determined a posteriori based on the crown-rump length as described (Noden and deLahunta 1985).

Human Subjects

Brain sections from human fetuses aged 16–17 weeks of gestation were obtained from the Department of Pathology of the Hospital Universitario La Paz in Madrid. Brains were removed in routine necropsies in accordance with the Spanish law on clinical autopsies (Boletín Oficial del Estado [BOE] of 27 June 1980 and BOE of 11 September 1982). After removal, brains were fixed by immersion in buffered 4% paraformaldehyde (PFA) at room temperature during 2 weeks. Then coronal blocks across the entire brain were obtained, these blocks were embedded in toto in paraffin, and finally sectioned and stained.

Viral Stocks

Two different *gfp*-encoding retroviruses were used in all cell lineage–tracing experiments: NIT-GFP (van Praag et al. 2002) and CAG–GFP (Zhao et al. 2006). Retroviruses were concentrated as described (van Praag et al. 2002) to working titers of 5×10^7 to 5×10^8 pfu/ml. The *gfp*-encoding adenovirus stocks were prepared as described (Borrell et al. 2006).

In Vivo Viral Injections and DNA Electroporation

Ferret kits were deeply anesthetized and maintained with 1.5% isoflurane during surgery. Pulled glass micropipettes were used for injecting 0.5 μl (postnatal day [P] 1 and P6) or 1 μl (P14) of retrovirus stocks to ferret kits aged P1 ($n = 4$), P6 ($n = 23$), and P14 ($n = 21$) or of adenovirus stocks to ferret kits aged P4 ($n = 2$) or P14 ($n = 2$). Adenovirus injections were aimed at the cortical plate (CP), and retrovirus injections were aimed at the OSVZ or ISVZ/VZ, by means of stereotaxic coordinates. Alternatively, cells in the VZ of the cerebral cortex were labeled by intraventicular injection of retrovirus-*gfp* or by electroporation of *dsred2*-encoding plasmids (Clontech) as previously described (Borrell 2010). Electroporated kits were aged P1 ($n = 11$) and P6 ($n = 13$). For double-labeling experiments, electroporation of DsRed2 plasmids into the VZ was immediately followed by injection of retrovirus-*gfp* into the OSVZ (P1, $n = 3$; P6, $n = 9$), as described above. After the appropriate survival period, kits were overdosed with sodium pentobarbital (Nembutal), perfused with PFA, and their brains processed as described below.

Binocular Enucleation

Enucleation was always performed bilaterally and on ferret kits aged P1. Kits were deeply anesthetized and maintained with 1.5% isoflurane during surgery. Eyelids were cut open, the connective tissue and muscle surrounding the eyeball were cut all around, the optic nerve severed, and the eyeball removed.

Bromodeoxyuridine Labeling and Tissue Collection

Bromodeoxyuridine (BrdU) (Sigma) was injected in ferret kits at P0, P2, P6, P10, P14, P20, or P30 ($n = 3$–5 animals per age) and in pregnant cats at 42 or 46 days of gestation ($n = 1$ pregnant female per age) at doses of 50 mg/kg body weight. For ferrets, 2 doses of BrdU were administered intraperitoneally 1 h apart. Two hours after the first BrdU injection, animals were overdosed with Nembutal and perfused transcardially with PFA. For cats, 1 dose of BrdU was administered intraperitoneally to pregnant damns. Two hours later, females were deeply anesthetized with ketamine/xylazine, embryos were obtained by caesarean section, and perfused transcardially with PFA.

Histochemistry, Immunohistochemistry, and In Situ Hibridization

For samples other than human, single and double immunostains were performed on 50-μm-thick free-floating sections. For the histochemical detection of acetylcholinesterase, sections were incubated in acetylcholine iodide and copper sulfate, then developed in sodium sulfur, enhanced with silver nitrate, and differentiated with sodium tiosulfate. For immunohistochemistry, sections were blocked and incubated in primary antibodies overnight at 4 °C. Primary antibodies and dilutions were as follows: anti-BrdU (1:100; Accurate); anti-phosphohistone 3 (1:1000; Upstate); anti-vimentin (1:400) and anti-Pax6 (1:1000; both from Chemicon); anti-Glial Fibrillary Acidic Protein (GFAP) (1:1000; DAKO); anti-DsRed (1:2000; BD Biosciences); rabbit anti-GFP (1:500; Molecular Probes) and chicken anti-GFP (1:1000; Aves); anti-caspase 3 (1:150; Cell Signaling), anti-Tbr2 (1:250; Abcam), anti-Olig2 (1:100; IBL), and anti-Ki67 (1:200; Novocastra). Sections were then incubated with appropriate fluorescently conjugated secondary antibodies (Chemicon and Jackson) and counterstained with 4′,6-diamidino-2-phenylindole (DAPI) (Sigma). Alternatively, sections were incubated with appropriate biotinylated secondary antibodies, with ABC complex (1:100; Vector) and developed with nickel enhancement as described elsewhere (Borrell et al. 1999). Where necessary, sections were counterstained with Nissl solution. For human samples, 6-μm-thick sections were obtained from paraffin blocks for histochemistry (hematoxylin–eosin or Nissl) and/or immunostain. After antigen retrieval, sections were incubated in primary antibodies, followed by incubation in biotinylated secondary antibodies, development with Dako REAL En Vision, and counterstain with Nissl. Primary antibodies were mouse monoclonal antihuman Ki-67 (Dako MIB-1), mouse monoclonal anti-vimentin (Progen VIM 3B4), and rabbit polyclonal antihuman synaptophysin (Dako A0010). In situ hybridization was performed as described elsewhere (Krishna et al. 2008).

Dye Tracing

Ferret kits aged P0, P2, P6, P10, and P14 ($n = 3$, 2, 3, 3, and 2, respectively) were perfused with phosphate-buffered 4% PFA and their brains stored in PFA at room temperature. Small crystals of DiI, DiD, and DiA (Molecular Probes) were delivered to the surface of the occipital cortex of developing ferret brains. Dyes were allowed to diffuse, while keeping the brains in PFA, between 2 months (younger animals) and 18 months (older animals), and then 60-μm-thick sections were obtained and counterstained with DAPI (Sigma). Images were captured by confocal microscopy (Leica).

Downloaded from https://academic.oup.com/cercor/article/21/7/1674/339599 by guest on 23 April 2024

Quantifications and Statistical Analysis

Determination of Cortical Layers

Layers of the developing cerebral cortex were identified and named following the terminology of the Boulder Committee (Boulder Committee 1970). The CP was considered for all ages as the cell-dense layer lying beneath the cell-sparse marginal zone (MZ), which at older ages also included the already distinguishable layers 5 and 6. The VZ was defined as the columnar epithelium of constant thickness lining the cortical ventricular wall and spanning up to a row of phosphohistone H3–positive (PH3+) nuclei, which marks the bottom limit of the SVZ (Bayer and Altman 1991; Brazel et al. 2003). In mouse and guinea pig, the SVZ was defined as a second cell-dense layer next to the VZ and below a cell-sparse layer. The intermediate zone (IZ) was defined as the cell-sparse layer found between the CP and the SVZ. In ferret, cat, sheep, and human samples, the cell-dense layer next to the VZ was identified as the ISVZ, and the cell-sparse layer between ISVZ and CP was further subdivided in a lower layer with a slightly higher cell density and containing large numbers of proliferating cells: OSVZ and an upper layer with a slightly lower cell density and with virtually no proliferating cells: IZ. The subplate was always included as part of IZ.

Determination of Area Borders

In juvenile ferrets (P20–P42), the positions of visual cortical areas A17, A19, and splenial visual cortex were determined as described (McConnell and LeVay 1986; Manger et al. 2002). In early postnatal ferret brains, the positions of the prospective A17 and A19 were approximated by comparison with their position in P14 subjects, with A17 usually defined as the dorso-occipital corner of the cerebral cortex and A19 as a neighboring area rostral to A17. In the youngest subjects, the identity of visual A17 was further confirmed by DiI retrograde tracing of axonal projections from neurons in the lateral geniculate nucleus (LGN). In cats, cortical regions were identified as parietal and temporal solely as a general topographical reference. In human fetal brains, lobes were identified according to Bayer and Altman (2005). Paracingular and parainsular regions were defined in coronal sections as those at the borders of the parietal lobe limiting with the prospective cingulated gyrus and insula, respectively. The cingulated region and the basal ganglia were distinguished from the paracingular and parainsular regions by the distinct cytoarquitecture of their neuroepithelium.

Gyrification Index

Gyrification index was defined and measured according to Zilles, as described (Zilles et al. 1988; Pillay and Manger 2007). For each species, measurements were made on images of 13 coronal sections evenly spaced along the entire rostrocaudal extent of the cerebral cortex. Images analyzed were from http://www.brainmuseum.org.

Cell Counts and Measurements

PH3+, Ki67+, BrdU+, or Nissl-stained cell nuclei were counted from rectangular sectors of cortex spanning its entire thickness, using Neurolucida (Microbrightfield) software coupled to a custom-made Matlab-based program. The contour of Nissl-stained cell somas was drawn using Neurolucida, and their size and density were calculated using Neurolucida Explorer (Microbrightfield).

Definition of IRGCs

Because the analysis of retrovirus-labeled GFP+ cells was done on 50-μm-thick sections, and the basal process of radial glia cells can be up to 3000 μm in length in the ferret, this process was frequently cut and unfortunately not all cells could be verified to contact the pial surface. For these reasons, GFP+ cells were considered IRGCs if they had one radial process extending for more than 80 μm in length toward the pial surface and also no apical process extended toward the ventricle. The average length of the radial process of these cells was 159.2 ± 8.8 μm (n = 91 cells), with examples 450-μm or 500-μm long, and they were clearly discernible from radially migrating neurons, which in the ferret we have measured to have a leading process of only 59.0 ± 0.8 μm in length (n = 289 cells).

Scaling of BrdU+ Nucleus Abundance

Monochrome microscopic images of BrdU stains were filtered through a Gaussian blur using a custom-made Matlab-based program, with the following values: sigma = 1, size = 5, and iterations = 20. Pixel density was then scaled linearly from 0 to 1 and pseudocolored.

Double-Labeling Analyses

Quantification of cell costaining was performed by confocal microscopy (Leica) through a ×40 lens and ×4 zoom. Images were acquired from cells in A17 from 4 sections per subject, 2–3 subjects per condition and age. Colabeling with PH3 was studied on cells in telophase. Images were analyzed using Imaris software (Bitplane).

Reconstruction of the Spread of Retrovirus-Labeled Cells in Mature Brain

DAPI and GFP fluorescence images were obtained from sections at representative lateromedial levels of injected brains. The GFP signal was monochromed, inverted, and digitized using Adobe Streamline software. The resulting dotted image was overlapped with the outer contours of layer I and white matter, drawn from the DAPI images.

Radial Glia Divergence Index

Each dye crystal deposited on the surface of the cerebral cortex (see above) labeled a small group of cell somas on the underlying ventricular surface. These somas belonged to radial glial cells whose radial fiber terminated at the site of dye crystal deposition. The distance between crystals of DiI and DiA placed on the surface of the brain was measured and defined the "MZ value"; the distance between cell somas labeled at the ventricular surface defined the "VZ value." The divergence index (DI) was defined as the ratio between the MZ and the VZ values. According to this formula, radial fibers running in parallel trajectories have a DI = 1. Fold values were calculated as the ratio between DI at each age over DI at P0.

Density of Radial Glial Fibers

Sagital brain sections 50-μm-thick were stained for anti-vimentin/DAPI and prospective cortical areas A17 and A19 identified. These were then scanned by confocal microscopy in *xz* mode, setting the *x* plane perpendicular to the trajectory of vimentin+ radial fibers. Density values were calculated as the number of vimentin+ circles (cross-sections of radial fibers) per unit of area of the *xz* cortical plane scanned (Gadisseux et al. 1992).

Expected Density of Radial Glial Fibers

This was defined as the density of radial glial fibers expected at each age if the changes in DI observed did not involve addition of new fibers and assuming isometric expansion of the cortical surface. Expected density was expressed as fold value with respect to P0 and calculated as the square of the ratio between DI at P0 over DI at each age.

Statistical Analysis

We used SPSS software to run the following tests where appropriate: independent samples or pairwise *t*-test, chi-quare test, or one-way analysis of variance followed by Bonferroni's test for multiple comparisons and Duncan's test for subset homogeneity.

Results

Widespread Existence of OSVZ among Gyrencephalic Mammals

Species in all major families of mammals develop cortical convolutions (Welker 1990). Thus, it is reasonable to propose that developmental mechanisms involved in such a complex morphogenetic process may be conserved across mammalian phylogeny. Current hypotheses point at progenitors in the OSVZ as playing critical roles in the expansion and folding of the cerebral cortex in primates, particularly humans (Smart et al. 2002; Zecevic et al. 2005; Kriegstein et al. 2006). To

Downloaded from https://academic.oup.com/cercor/article/21/7/1674/339599 by guest on 23 April 2024

understand the developmental mechanisms responsible for the tangential expansion and folding of the cerebral cortex in mammals, we began by studying and comparing the patterns of progenitor proliferation in the embryonic cerebral cortex of both lissencephalic and gyrencephalic species, at equivalent stages of cortical development (peak of neurogenesis for layer 2/3). Species were selected to represent 4 of the major families of extant mammals: rodents, primates, ungulates, and carnivores. Mouse embryos of 15.5 days of embryonic development (E15.5) had most cortical progenitors dividing in the VZ, few in the SVZ, and virtually none elsewhere, as identified by detection of the mitotic marker PH3 and the cell cycle–specific antigen Ki67 (Fig. 1*A,B* and Supplementary Fig. S1 and Table S1). In the cerebral cortex of E30 guinea pig embryos (another lissencephalic rodent), virtually all progenitors accumulated in the VZ and SVZ, with only a few cells found in the lower IZ next to the SVZ (4.8 ± 0.8%, mean ± standard error of the mean) (Fig. 1*A,B* and Supplementary Fig. S1 and Table S1). Intriguingly, the proportion of progenitors located in the different layers varied between cortical regions, but the general patterns were robustly conserved (Supplementary Fig. S2). In human fetuses of 16–17 weeks of gestation, on the other hand, cycling progenitors were most abundant in the OSVZ (63.8 ± 5.3%), as identified with anti-Ki67 antibodies (Fig. 1*A,B* and Supplementary Fig. S2 and Table S1). These observations were in agreement with previous descriptions of both mouse and human cortical development and so far supported the current view that the OSVZ is a feature unique to primates (Smart et al. 2002; Zecevic et al. 2005; Dehay and Kennedy 2007; Hansen et al. 2010).

Because the OSVZ houses the majority of intermediate progenitors in primates, this is hypothesized to play a central role in cortical expansion and folding in these species (Kriegstein et al. 2006; Dehay and Kennedy 2007). We

Downloaded from https://academic.oup.com/cercor/article/21/7/1674/339599 by guest on 23 April 2024

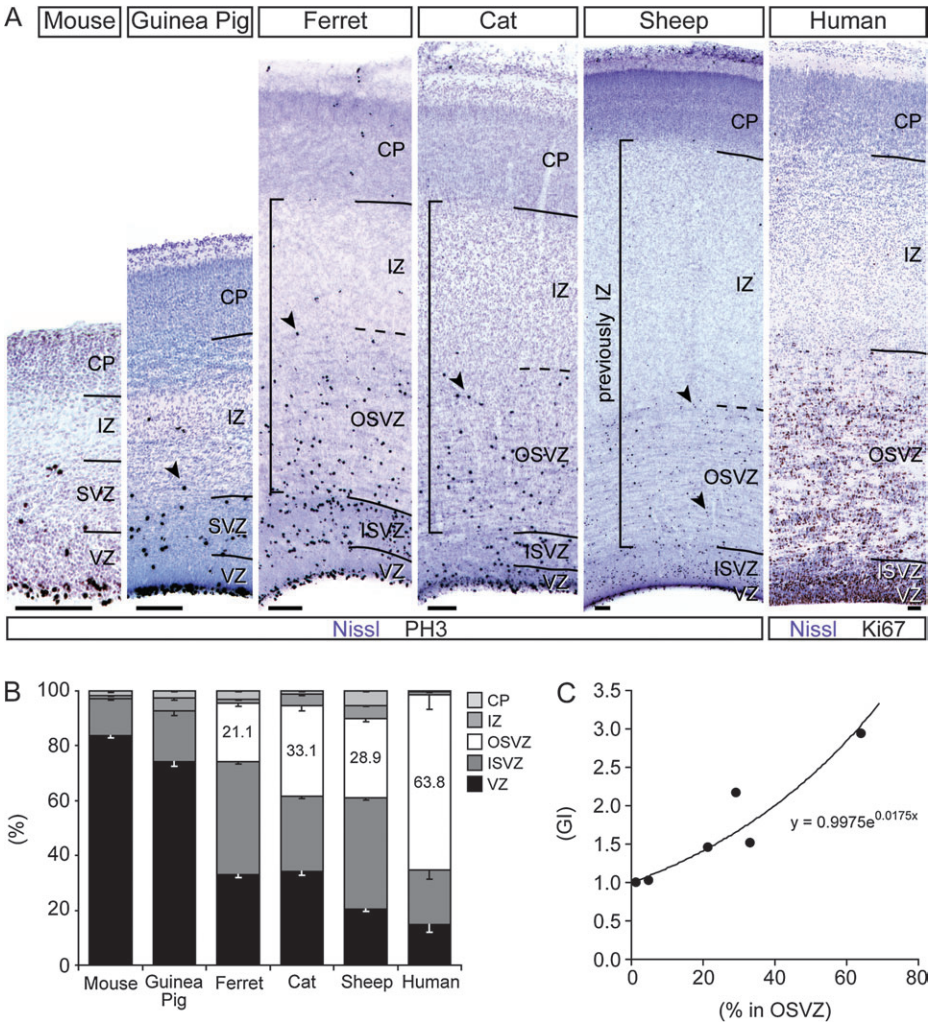

Figure 1. OSVZ progenitors are found in the developing cerebral cortex of gyrencephalic mammals. (*A*) Distribution of progenitor cells in the cerebral cortex of lissencephalic and gyrencephalic mammals at equivalent developmental stages revealed by the detection of PH3 (mouse, E15.5; guinea pig, E30; ferret, P0; cat, E46; sheep, E65) or Ki67 (human, 16 gestational weeks) on coronal sections at equivalent levels. Note that in the gyrencephalic species labeled cells accumulate in 2 cell-dense layers plus an additional cell-sparse layer, reminiscent of the human VZ, ISVZ, and OSVZ (arrowheads), respectively. In guinea pig, a small number of progenitors are located in the lower aspect of the IZ. In human, the layer labeled as IZ also includes the subplate. (*B*) Quantification of the distribution of progenitor cells across the layers of the developing cerebral cortex in each of the species studied. Numbers indicate the percentage of progenitors located in the OSVZ (mean ± standard error of the mean); $n = 2$ fields per section, 3–4 sections per embryo, and 2–4 embryos per group. (*C*) Plot of the relationship between percentage of progenitors in OSVZ (gyrencephalic species) or IZ (lissencephalic species) and the gyrification index (GI) for each species. The best-fit exponential curve is indicated and plotted, which has a correlation coefficient of $r^2 = 0.881$, and a statistical significance of $P < 0.01$ (*t*-test). Scale bar—100 μm.

reasoned that, by extension, an OSVZ should also exist in the developing cerebral cortex of nonprimate gyrencephalic mammals. Upon examination of the developing cerebral cortex of ferret, cat, and sheep specimens, we found a very abundant population of progenitor cells in the lower half of a layer so far identified as IZ in these species (Jackson et al. 1989; Noctor et al. 1997; Martinez-Cerdeno et al. 2006) (Figs 1*A*,*B* and 2*A*, and Supplementary Figs S1 and S2 and Table S1). Because the consensus nomenclature defines the IZ as a nonproliferative layer (Boulder Committee 1970; Bystron et al. 2008), our results strongly suggested that this proliferative compartment should not be included as part of the IZ. Moreover, the location of this compartment between the SVZ and IZ, together with its high abundance of progenitor cells, suggested that this layer might be a vestigial form of the primate OSVZ. Therefore, we defined the OSVZ in nonprimate species as a cell-sparse but highly proliferative layer located between the cell-dense proliferative ISVZ and the cell-sparse nonproliferative IZ (Figs 1*A* and 2*A*).

In order to determine if the newly identified progenitors were equivalent to primate OSVZ progenitors, we focused on the ferret and performed an extensive marker expression

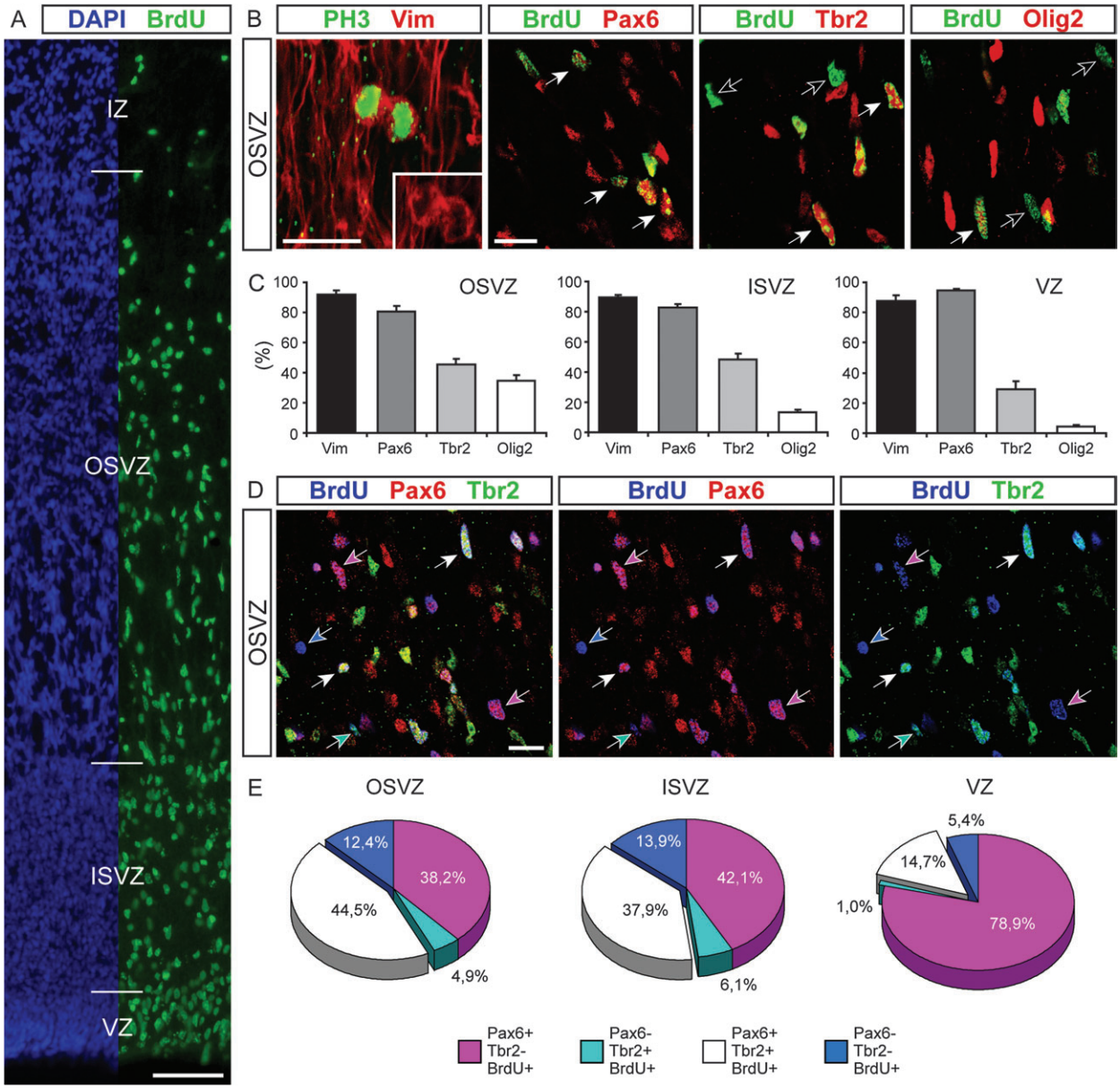

Figure 2. Cortical progenitors in the developing ferret cerebral cortex are very heterogeneous. (*A*) Density and distribution of BrdU-incorporating progenitors (green) in the VZ, ISVZ, and OSVZ of ferret cerebral cortex at P6. Layer boundaries are delineated with DAPI stain (blue). (*B*) Analysis of marker expression of OSVZ progenitors in the occipital cortex of ferret at P6. Progenitors are identified by PH3 or BrdU stains (green). Progenitors positive or negative for the markers are indicated by solid or open arrowheads, respectively. (*C*) Quantification of the percentage of progenitors in the different layers positive for each of the markers (mean ± standard error of the mean); $n = 3$ sections per animal and 3 animals per group. (*D*) Multiple-marker analysis of OSVZ progenitors in the occipital cortex of ferret at P6. Progenitors are identified by BrdU stain (blue), Pax6+ cells are in red, and Tbr2+ cells are in green. Progenitor cells positive for one, both, or none of the markers are indicated by color-coded arrows according to the legend in (*E*). (*E*) Quantification of the percentage of progenitors in the different proliferative layers positive for each of the marker combinations indicated in the legend; $n = 3$ sections per animal and 3 animals per group. Scale bars—(*A*): 100 μm; (*B*, *D*): 15 μm.

Downloaded from https://academic.oup.com/cercor/article/21/7/1674/339599 by guest on 23 April 2024

analysis. We started with vimentin, an intermediate filament typically expressed by radial glia cells in carnivores and humans (Engel and Muller 1989; Voigt 1989; Honig et al. 1996). We found that in the ferret 91.9 ± 2.8% of mitotic cells in OSVZ expressed vimentin (Fig. 2*B,C* and Supplementary Table S2), which in human this was observed in 92.6 ± 1.95% of OSVZ mitoses (n = 362 cells, 5 fetuses; Supplementary Fig. S5). Analysis of transcription factor expression in cycling progenitors (as identified by incorporation of BrdU) showed that in ferret about 81% of OSVZ progenitors expressed Pax6 (Fig. 2*B,C* and Supplementary Table S2). This was very similar to data from human and macaque OSVZ, where 80–90% of progenitors have been reported to express Pax6 (Bayatti et al. 2008; Fish et al. 2008; Mo and Zecevic 2008; Hansen et al. 2010) and completely different from mouse SVZ, where Pax6 is virtually never expressed (Kowalczyk et al. 2009). The T-box transcription factor Tbr2 was expressed by only 45% of OSVZ progenitors (Fig. 2*B,C* and Supplementary Table S2), similar to the 43% of OSVZ progenitors in human (Bayatti et al. 2008; Hansen et al. 2010), whereas in the mouse it is expressed by 98% of SVZ progenitors (Englund et al. 2005). When analyzed simultaneously, we found that on average Pax6 and Tbr2 were coexpressed by 44% of OSVZ progenitors, whereas expression of Pax6 alone was found in 38% of progenitors and Tbr2 alone in only 5% (Fig. 2*D,E* and Supplementary Table S2). This was again similar to data reported on human OSVZ (Mo and Zecevic 2008; Hansen et al. 2010) and completely different than in the mouse, where Pax6 and Tbr2 are virtually never coexpressed (Englund et al. 2005; Kowalczyk et al. 2009). Olig2, a transcription factor that in the cerebral cortex is typically expressed by oligodendroglial progenitors (Tekki-Kessaris et al. 2001; Mo and Zecevic 2009), was expressed by about 34% of OSVZ progenitors in ferret (Fig. 2*B,C* and Supplementary Table S2), remarkably similar to the human SVZ, where 35% are oligodendrocyte progenitors (Zecevic et al. 2005). Next we extended these analyses of transcription factor expression to the ISVZ and VZ, as distinguished cytoarquitectonically (Fig. 2*A*). The molecular profiling of progenitors in the ISVZ was remarkably similar to that in the OSVZ, both considering each of the markers alone and in combination (Fig. 2). In contrast, in the VZ much fewer progenitors expressed Tbr2 or Olig2 (Fig. 2*C*), and the vast majority expressed Pax6 alone (Fig. 2*E*). Interestingly, a common feature for all germinal layers was that a great majority of Tbr2+ progenitors coexpressed Pax6, whereas only half or less of Pax6+ progenitors coexpressed Tbr2 (Fig. 2*E*).

Finally, to examine if the differences in abundance of OSVZ progenitors between mammalian species might relate to their different degrees of cortical convolution in the mature brain (Zilles et al. 1988; Pillay and Manger 2007), we examined if there was a scaling relationship between these 2 factors. We found that linear increases in the proportion of progenitors in the embryonic OSVZ (or IZ for lissencephalic species) had a statistically significant correlation with exponential increases in the gyrification index of the adult cortex (Fig. 1*C*; $r^2 = 0.881$, $P < 0.01$). Taken together, these results showed that the existence of OSVZ as a distinctive germinal layer is a feature common to all gyrencephalic mammals examined and not exclusive to primates. Our analyses also showed that these progenitors are qualitatively different than the SVZ progenitors in lissencephalic species but similar to the OSVZ progenitors in primates and strongly suggested that their relative abundance may be relevant for the degree of expansion and folding of the cerebral cortex.

Patterned Distribution of Cortical Progenitors Precedes the Patterned Expansion of the Cortical Mantle

In order to define the contribution of the various progenitor populations to the expansion and folding of the cortical mantle, we took advantage of the fact that different territories of the cerebral cortex undergo different degrees of expansion and folding during development. In the ferret cerebral cortex, for example, 2 of the folds outstand for their large surface area: the splenial gyrus (SG) and the double sigmoid system (SS), which are flanked by some of the deepest fissures (Fig. 3*A–C*) (Smart and McSherry 1986a, 1986b). First, we studied the distribution of cycling progenitors across the developing ferret cerebral cortex by short-pulse BrdU labeling. Between P0 (newborn) and P14, BrdU+ progenitors were particularly abundant in cortical territories known to undergo a dramatic expansion: the most rostral and caudal regions (prospective sigmoid and SG, respectively). Comparatively fewer BrdU+ cells were observed in neighboring regions (Fig. 3*D,E* and Supplementary Figs S3 and S4). Next, we focused on the caudal region, containing the SG that includes visual area (A) 17 and the lateral sulcus that includes area A19 (Fig. 3*C*). We found that the abundance of BrdU+ cells was greater in the prospective SG (A17) than in the prospective lateral sulcus (A19), with changes appearing most dramatic in the OSVZ and to a lesser extent in the ISVZ and VZ (Fig. 3*F–L*). Quantification of PH3+ cells demonstrated that the density of mitoses was 1.4–1.6-fold higher in the VZ of the prospective A17 than in A19 between P0 and P6, as well as in the ISVZ between P2 and P10 (Fig. 3*H*). Most significantly, the density of mitoses in the OSVZ was 2- to 4-fold higher in the prospective A17 versus A19 (Fig. 3*H*). These findings demonstrated that progenitors are not evenly distributed across the developing cortex and that these accumulate specifically in regions that will undergo the greatest tangential expansion.

To determine if our observations in ferret might be indicative of a general feature among gyrencephalic species, we also investigated the patterns of proliferation in the developing cerebral cortex of cat and human. In cat, the parietal region of the cerebral cortex has a higher degree of folding and greater surface area expansion than the temporal region (Supplementary Fig. S5). Between E42 and E46 (stages equivalent to P0–P4 in ferrets [Issa et al. 1999]), when the cerebral cortex of cat embryos still shows no signs of gyration, the density of PH3+ cells was higher in the prospective parietal than temporal cortex, particularly in the OSVZ where differences were 3- to 4-fold (Supplementary Fig. S5). In human, the parietal and temporal lobes are regions where the cerebral cortex displays a dramatic degree of tangential expansion and folding, as opposed to the insular and cingulated regions, where the cerebral cortex expands comparatively little during embryogenesis (Supplementary Fig. S5). At 16–17 weeks of gestation (stages of cortical development presumed equivalent to P6–P10 in ferrets [Rakic 1995a; Issa et al. 1999]), the density of proliferative progenitors (Ki67+ cells) in the OSVZ was about 2-fold higher in the prospective parietal and temporal cortex than in the prospective paracingular and parainsular regions (Supplementary Fig. S5). Taken together, our results demonstrated that,

Downloaded from https://academic.oup.com/cercor/article/21/7/1674/339599 by guest on 23 April 2024

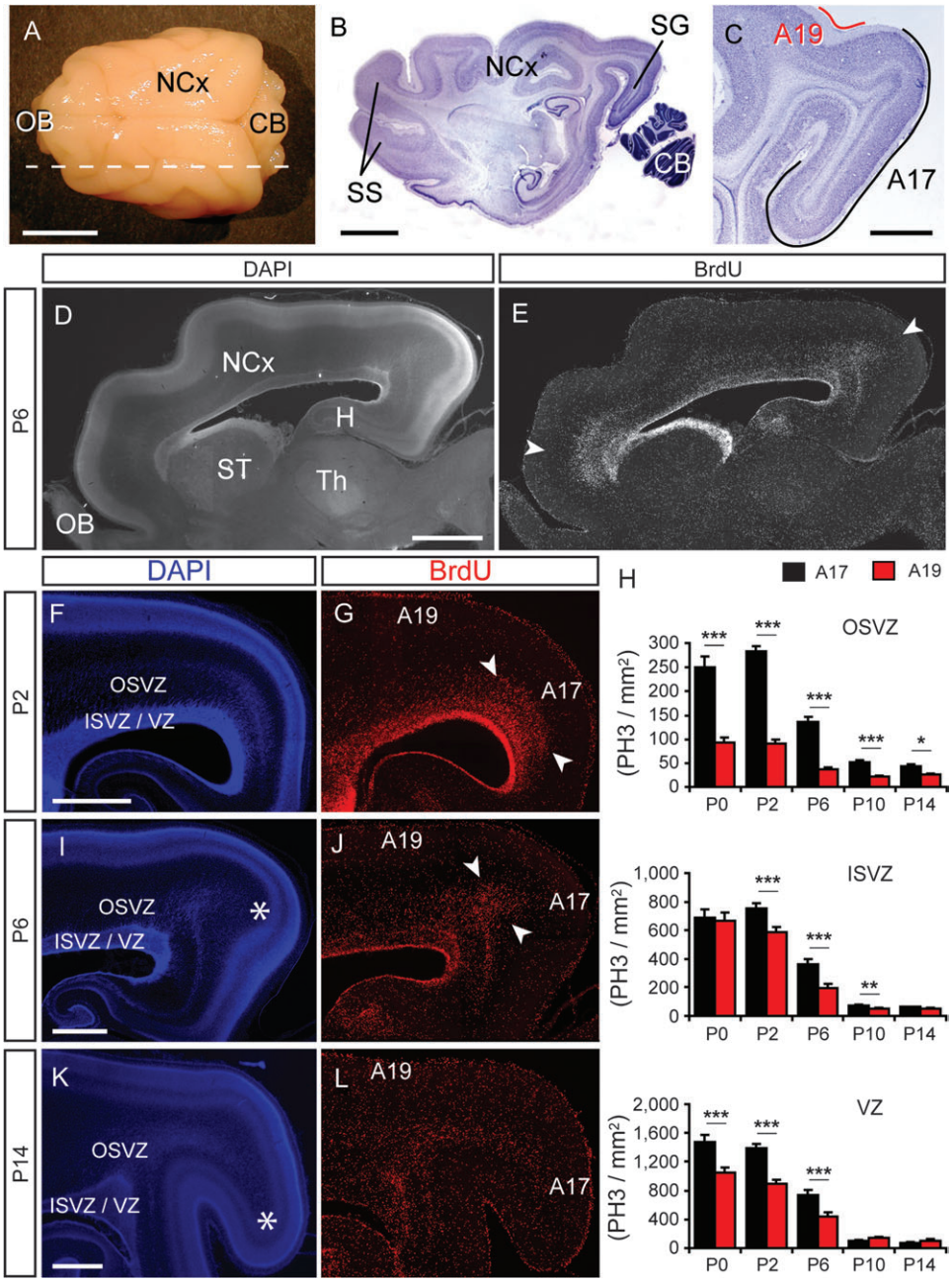

Figure 3. Local differences in OSVZ progenitor density across the cerebral cortex correlate with region-specific tangential expansion. (*A–C*) Cerebral cortex of a P30 ferret seen externally (*A*) and in sagital sections (*B*, *C*), showing the SG, which contains visual area A17 and is flanked by a sulcus containing A19, and the SS. (*D*, *E*) Distribution of BrdU-incorporating progenitors at P6, which accumulate in the frontal and occipital cortex of the ferret (arrowheads). (*F–L*) Distribution of BrdU+ progenitors and dividing cells in the ferret occipital cortex between P2 and P14. Progenitors (red) accumulate in the OSVZ of the prospective A17 (asterisk) at P2 and P6 (*G*, *J*, arrowheads). (*H*) Quantification of density of PH3+ progenitors in the OSVZ, ISVZ and VZ of prospective A17 and A19 at the ages indicated (mean ± standard error of the mean); $n = 1$ field per section, 3–4 sections per animal, and 3–5 animals per group. $^{*}P < 0.05$, $^{**}P < 0.01$, $^{***}P < 0.001$; pairwise *t*-test. CB, cerebellum; H, hippocampus; NCx, neocortex; OB, olfactory bulbs; ST, striatum; TH, thalamus. Scale bars—(*A*): 1 cm; (*B*) 5 mm; (*C–E*): 2 mm; (*F*, *G*, *I–L*): 1 mm.

for a number of gyrencephalic species, the patterned distribution (or differential abundance) of cortical progenitors, and particularly those in the OSVZ, precedes the expansion of the cortical mantle following identical patterns. These findings thus supported the hypothesis that in gyrencephalic species the expansion in surface area of the cerebral cortex may rely, at least in part, on the occurrence of high levels of cell proliferation at the OSVZ.

Extensive Tangential Dispersion of Cortical Pyramidal Neurons

We next investigated the fate and pattern of dispersion of cells born from OSVZ, ISVZ, and VZ progenitors. For this, we focused again on the postnatal development of the SG (A17) of the ferret, where neurogenesis for layer 2/3 spans the entire first postnatal week and declines rapidly after P8 (Jackson et al. 1989). The lineage of OSVZ and ISVZ progenitors was labeled

Downloaded from https://academic.oup.com/cercor/article/21/7/1674/339599 by guest on 23 April 2024

by focal injection of retrovirus-*gfp*, and the lineage of VZ progenitors was labeled by electroporation of a *dsred*-encoding plasmid (Borrell 2010). VZ progenitors produced vast numbers of layer 2/3 pyramidal neurons during the first postnatal week (Fig. 4*A–B*) (Borrell 2010). ISVZ progenitors could only be labeled specifically after P14, when they generated some additional pyramidal neurons but mainly produced glial cells

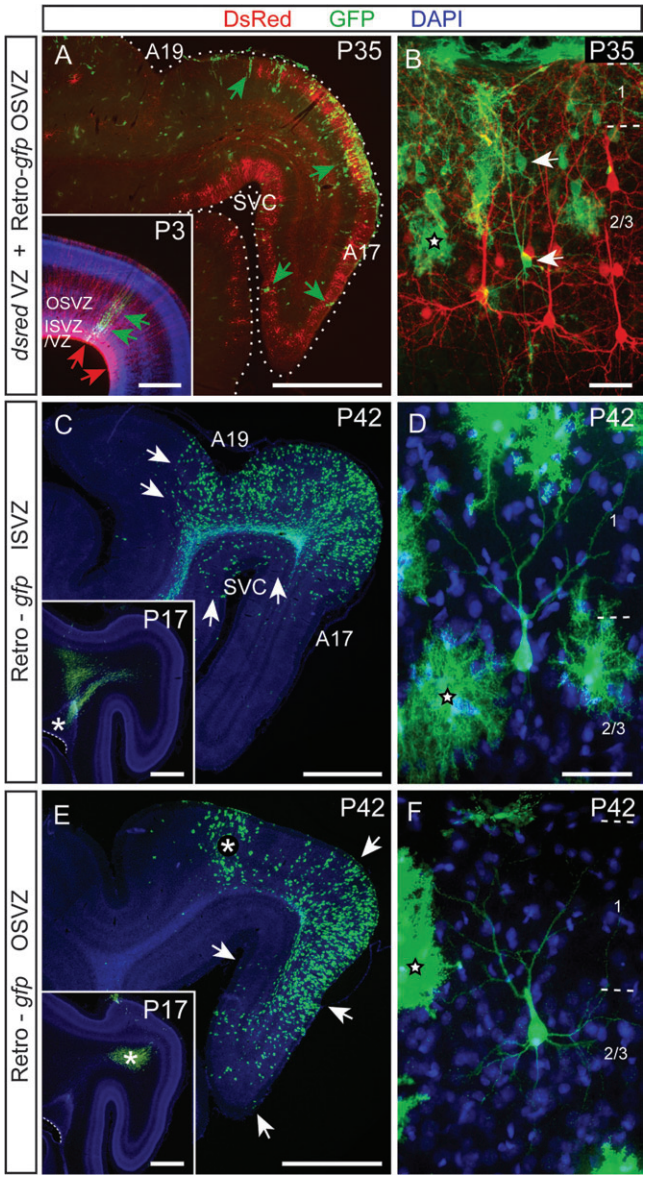

Figure 4. OSVZ progenitors generate neurons and glia that undergo dramatic tangential dispersion. (*A*, *B*) Fate and tangential dispersion of cells born from *dsred*-electroporated VZ progenitors (inset in [*A*], red arrows) and from retrovirus-*gfp*–infected OSVZ progenitors (inset in [*A*], green arrow) at P1. Cells from a small domain of OSVZ (green) disperse over the entire SG (*A*, arrows). Pyramidal neurons generated by VZ progenitors (red) next to pyramids (arrows) and astrocytes (star) generated by OSVZ progenitors (green) (*B*). (*C–F*) Fate and spreading pattern of cells born from progenitors in the ISVZ/VZ (*C*, *D*) or OSVZ (*E*, *F*) of prospective A17 labeled by local injection of retrovirus-*gfp* at P14 (insets, asterisk). Cells from the ISVZ/VZ (*C*) spread throughout the gyrus and flanking fissures (arrows in *C*). Cells from the OSVZ (*E*) populated the entire gyrus (arrows) but never the flanking fissures. Asterisk in (*E*) marks the tract of the injection pipette. Astrocytes (stars) and layer 2/3 pyramidal neurons derived from ISVZ/VZ (*D*) and OSVZ (*F*) progenitors. Scale bars—(*A*, *C*, *E*): 2 mm; inset in (*A*): 500 μm; insets in (*C*, *E*): 1 mm; (*B*): 50 μm; (*D*, *F*): 30 μm.

(Fig. 4*C–D*). Cells derived from OSVZ progenitors followed both neuronal and glial lineages at all ages examined (Fig. 4*B,F* and Supplementary Fig. S6), which is consistent with previous studies in human demonstrating that progenitors in the OSVZ span a wide range of potentialities including the generation of neurons, astrocytes, and oligodendrocytes (Mo et al. 2007; Mo and Zecevic 2009; Hansen et al. 2010). However, whereas studies in human and macaque have shown that a large proportion of OSVZ progenitors are neurogenic (Lukaszewicz et al. 2005; Dehay and Kennedy 2007; Mo et al. 2007; Mo and Zecevic 2008; Hansen et al. 2010), we systematically observed that OSVZ progenitors in ferret contributed to the mature cerebral cortex with many more astrocytes than neurons.

Regarding patterns of dispersion, although retrovirus injections in the ISVZ and OSVZ were small and only affected progenitors within a small area (Fig. 4*A,C,E* and Supplementary Fig. S7), neurons and astrocytes derived from such small cluster of progenitors were consistently found spread over several millimeters of cerebral cortex, to cover the entire extent of the SG (Fig. 4*A,E* and Supplementary Fig. S8). These results demonstrated that pyramidal neurons and other cells derived from ISVZ and OSVZ progenitors had undergone extensive tangential dispersion during the process of radial migration.

Progressive Divergence of Radial Glia Fibers during Gyrus Formation

The patterns of cell dispersion described above posed the following topological problem: since cortical neurons follow the fibers of radial glia for their radial migration to the cortical surface, the tangential scatter of pyramidal neurons within the cerebral cortex is limited by the trajectory of the fibers of radial glia between their site of birth and their final location (Rakic 1995a; Noctor et al. 2004; O'Leary and Borngasser 2006). Hence, in order for locally generated neurons to spread to the whole extent of the SG, an array of radial glia fibers should exist to support it (Fig. 5*K*). To address this issue, we first performed experiments in the prospective SG of ferrets (A17), where we injected lipophilic tracers on the surface of the cerebral cortex to trace radial glia cells from the tips of their radial fiber at the pial surface, to the cell soma at the ventricular surface. At all ages examined, we found that radial glia fibers followed divergent trajectories across the cortical thickness, establishing a fanned array of radial fibers (Fig. 5*A–C*). The degree of radial fiber divergence, expressed as DI, increased exponentially during the first postnatal weeks (P0, DI = 3.1 ± 0.4; P14, DI = 23.7 ± 2.3) (Fig. 5*D,J*). Similar DI values were obtained by reconstruction of radial fiber trajectories on sections stained with anti-vimentin antibodies (P0, DI = 3.2 ± 0.1; P6, DI = 4.7 ± 0.3). These values were 3- to 8-fold higher than reported in mice at comparable stages (E14, DI = 1.3; P0, DI = 3.15; [Gadisseux et al. 1992]). Our analyses also revealed that in the prospective lateral sulcus (A19), in contrast, radial fibers followed largely parallel trajectories (P0, DI = 1.3 ± 0.1; P6, DI = 1.4 ± 0.1).

The developmental increase in divergence between radial fiber trajectories in the expanding gyrus suggested that the density of these radial fibers at the cortical surface might decrease in a similar degree in this region. Based on our measurements of radial glia divergence, we estimated a theoretical reduction on radial fiber density of 60-fold between P0 and P14 (Fig. 5*J*). However, actual measurements of radial fiber density at the top of the CP demonstrated only a 1.4-fold

Downloaded from https://academic.oup.com/cercor/article/21/7/1674/339599 by guest on 23 April 2024

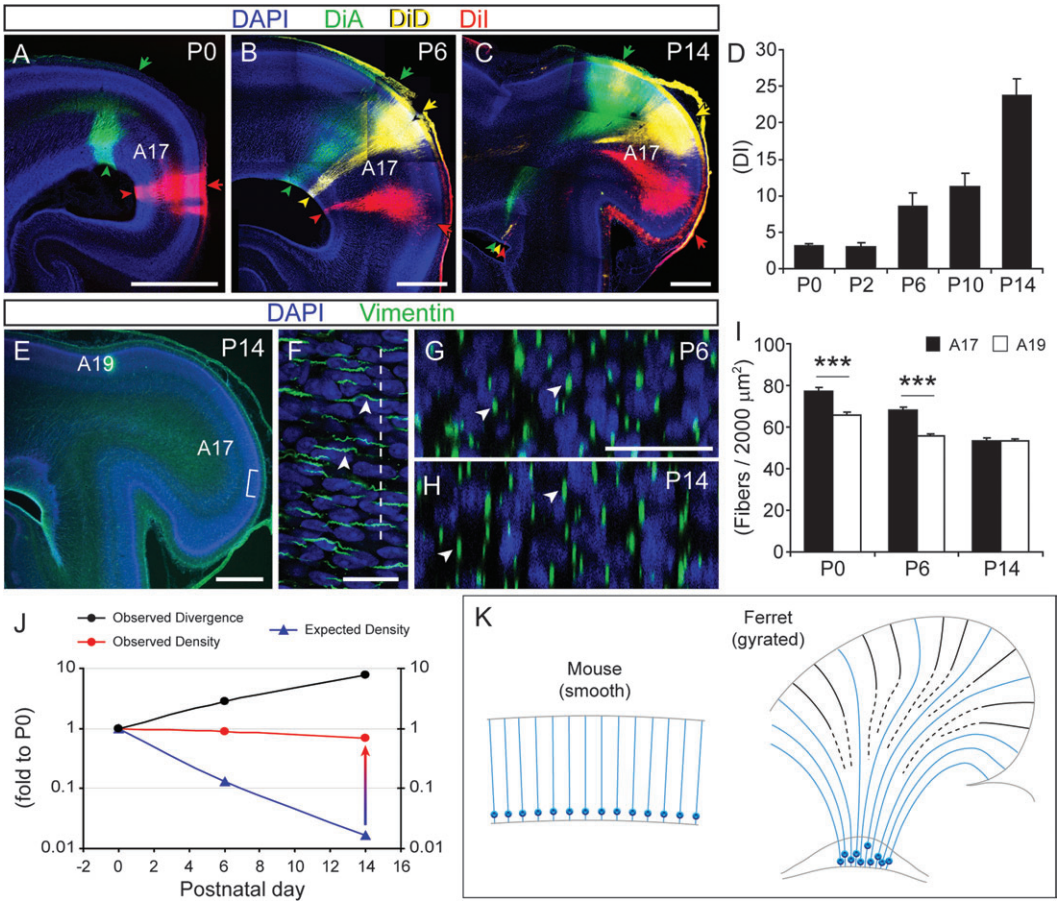

Figure 5. Radial glia fibers follow increasingly divergent trajectories during gyrus formation. (*A–C*) Dye tracing of radial glia fibers in the prospective A17 of postnatal ferrets. Colored arrows indicate sites of crystal deposition, and arrowheads indicate the location of retrogradely labeled radial glia cell somas at the ventricular surface. (*D*) Degree of divergence of radial glia fiber trajectories measured as DI (mean ± standard error of the mean); $n = 2$–3 animals per group. (*E–H*) Anti-vimentin stains revealing radial glia fibers. Bracket in (*E*) indicates area shown in (*F*). (*F*) Confocal image showing radial fibers (green, arrowheads) in the CP. Dashed line indicates orientation of images shown in (*G*, *H*). (*G*, *H*) Confocal images of brain sections as in (*F*), scanned orthogonal to the trajectory of radial fibers. Green dots are cross-section views of radial fibers (arrowheads), and cell nuclei are in blue. (*I*) Quantification of density of vimentin+ fibers at the top of the CP in A17 and A19 between P0 and P14 (mean ± standard error of the mean); $n = 12$ fields per animal and 3 animals per group; $^{***}P < 0.001$, pairwise *t*-test. (*J*) Representation of the DI of radial fibers (black dots), observed (red dots) and expected (blue triangles) density of vimentin+ radial fibers at the cortical surface, along the period of SG development, expressed as fold change with respect to values at P0. By P14, the observed radial fiber density, and hence the total number of radial fibers, is 60-fold greater than expected (colored arrow). (*K*) Schematic drawing illustrating differences in the radial fiber scaffold between species with a smooth cortex and those with a gyrated cortex. Whereas in the mouse cerebral cortex radial glia fibers (blue lines) follow parallel trajectories, in the ferret these are highly divergent in gyrated areas (blue lines). In spite of their divergence, the density of radial fibers at the CP does not change, indicating the existence of additional radial fibers (black lines). Scale bars—(*A–C*, *E*): 1 mm; (*F–H*): 30 μm.

decrease in radial fiber density during that period (Fig. 5*E–I*), which represented a reduction in the number of radial fibers 42 times smaller than our estimated 60-fold reduction (Fig. 5*I*). This indicated that additional fibers were being incorporated into the radial glia fiber scaffold as the cortical gyrus expanded. Taken together, these results demonstrated that the scaffold of radial fibers was progressively diverging as the surface of the cerebral cortex expanded and also that these dramatic increases in radial fiber divergence did not lead to equivalent reductions in radial fiber density (Fig. 5*J*,*K*). This indicated that the absolute number of radial fibers reaching the CP increased very dramatically during this developmental period.

OSVZ Includes a Specialized Type of Progenitor Cell: Intermediate Radial Glia

The above analysis of the radial fiber system strongly suggested that during cortical expansion many additional radial fibers are being intercalated into the preexisting scaffold (Fig. 5*K*, black lines). We reasoned that one possibility is that new fibers might be produced by the branching of preexisting fibers of radial glia cells. Previous studies have shown that in the neocortex of mouse and macaque monkey, the fibers of radial glia can branch, although this was interpreted as the mechanism for transformation of the simple fiber of radial glia into the elaborate arborization of astrocyte processes (Schmechel and Rakic 1979a; Takahashi et al. 1990). In the case of gyrencephalic brains, collateral branching of radial glia fibers could potentially contribute to the increase in the total number of radial fibers and, more importantly, to the progressive divergence of the radial fiber scaffold (Fig. 5*K*). To achieve this, however, radial fiber branching would have to be really exuberant, with an estimated average of 42 collateral branches per radial fiber (see above). If this was the case, our dye-labeling experiments would most likely reveal cells colabeled with 2 dyes (see Fig. 5*B*,*C*), which never occurred regardless of the proximity between labeled cells ($n = 13$ animals).

An alternative hypothesis would be that OSVZ progenitors in gyrencephalic mammals generated additional, but specialized,

Downloaded from https://academic.oup.com/cercor/article/21/7/1674/339599 by guest on 23 April 2024

radial glia cells. In this scenario, new radial glia cells would extend additional, intercalated, radial fibers to the cortical region undergoing expansion. This would provide radially migrating neurons with a fanned array of radial trajectories, enabling them to spread tangentially throughout the CP. Furthermore, at late stages when neuronal migration is complete, OSVZ-generated radial glia cells would also migrate radially and terminally differentiate into astrocytes (Schmechel and Rakic 1979a; Voigt 1989; deAzevedo et al. 2003; Rakic 2003a), which they would do also in a fanned array, and end-up populating the entire expanded cortical area as we have observed (Fig. 4 and Supplementary Fig. S8). The first evidence in favor of this hypothesis was that the vast majority of mitotic cells in the OSVZ of ferret, cat, and human were positive for vimentin (demonstrated to be a general marker of radial glia cells in carnivores and humans [Engel and Muller 1989; Voigt 1989; Honig et al. 1996]; Fig. 2*B,C* and Supplementary Fig. S5). Second, we injected retrovirus-*gfp* in the OSVZ of the prospective SG of early postnatal ferrets as before but allowing only 2 days of survival in order to visualize the detailed morphology of cells generated from recent local divisions. We found many GFP+ cells bearing morphology typical of radial glia, with a thin process extended radially, branched at the MZ and ending at the pial surface with end-feet (Fig. 6*A,B* and Supplementary Fig. S7). Although the radial process of these cells could not always be followed up to the pial surface due to tissue processing limitations (Supplementary Fig. S7), these processes were always unmistakably longer than the leading process of migrating neurons (radial glia-like cells: 159.2 ± 8.8 μm, $n = 91$ cells; radially migrating neurons in ferret: 59.0 ± 0.8 μm, $n = 289$ cells; $P < 10^{-18}$) (Borrell et al. 2006; Borrell 2010). In contrast to classical radial glia cells, which extend an apical process to the ventricular surface (Supplementary Fig. S6), these cells ended freely within the OSVZ, without an apical process contacting the ventricular surface (Fig. 6*B,B′*). Anti-vimentin stains demonstrated that 71% of these cells were vimentin+ ($n = 48$ cells; Fig. 6*D,D′*) and that cells with identical morphological and immunological characteristics also exist in the OSVZ of developing human embryos (Fig. 6*I*), as also described by others (Sidman and Rakic 1973; deAzevedo et al. 2003; Rakic 2003b; Hansen et al. 2010).

Retrovirus-encoded DNA is stochastically integrated into the genome of only 1 of the 2 cells after the first mitosis, so if the division is asymmetric, a retrovirus will label the mother cell 50% of the times. Since classical radial glia is acknowledged to be the main neurogenic progenitor in the cerebral cortex and, late in development, to be the main astrocytic progenitor [reviewed in Rakic 2003a), we wanted to understand if these cells with features of radial glia could also be progenitors, and in that case distinguish if they were neurogenic, astrocytogenic, or self-amplifying. To this aim, we classified GFP+ cells in the OSVZ as exhibiting radial glia-like morphology or not (Fig. 6*A–C*). Nonradial glia-like cells usually had multipolar morphology, typical of developing astrocytes, or bipolar morphology, typical of migrating neurons. In the OSVZ of P1:P3 ferret kits (infected with retrovirus at P1, analyzed at P3), 70.4 ± 3.3% of GFP+ cells had radial glia-like morphology (Fig. 6*C*); in P6:P8 subjects radial glia-like cells were 50.7 ± 3.9% of GFP+ cells ($n = 702$ cells, 6 animals); and in P14:P17 ferrets these were only 13.7 ± 6.4% ($n = 851$ cells, 3 animals). Therefore, since more than 50% of GFP+ cells in the OSVZ had radial glia-like morphology in P1:P3 kits, this strongly suggested that during that period progenitors in the OSVZ of the ferret SG included not only neurogenic or astrocytogenic progenitors but also a population of self-amplifying radial glia-like progenitors.

Unfortunately, in P1 ferret surgeries, it was not technically possible to avoid the spread of retrovirus infections beyond the injection site, and a small amount of GFP+ cells was also observed in the ISVZ and VZ (Fig. 6*A* and Supplementary Fig. S7). Morphological analysis of these cell populations in P1:P3 ferrets revealed that 45.4 ± 4.0% of cells in the ISVZ had radial glia-like morphology, 87.2 ± 1.1% of GFP+ cells in the VZ had classical radial glia morphology, and the remaining cells had multipolar morphology (Fig. 6*A,C*). These results suggested the possibility that maybe the GFP+ radial glia-like cells in the OSVZ were not originated locally by self-amplifying radial glia-like progenitors but rather were "displaced radial glial cells" that had translocated from the VZ, as argumented in earlier studies (Ramon y Cajal 1891; Sidman and Rakic 1973; Choi and Lapham 1978; Schmechel and Rakic 1979b; Voigt 1989; deAzevedo et al. 2003; Noctor et al. 2004; reviewed in Rakic 2003a, 2003b). In order to determine if OSVZ radial glia-like cells originate directly from VZ radial glia progenitors, we injected retrovirus-*gfp* in the telencephalic ventricle of P1 ferrets and analyzed the resulting labeled cells at P3, a timing exactly like in our previous retrovirus injections in the OSVZ (see above). Out of 218 GFP+ cells evaluated from 3 animals, 138 cells were located in the VZ (63.3%), 79 cells were in the ISVZ (36.2%), and only 1 cell was found in the OSVZ (0.5%), which displayed multipolar morphology (Fig. 6*E*, open arrowhead). This result clearly refuted the possibility that the large numbers of radial glia-like cells we had observed in the OSVZ could be displaced radial glial cells from the VZ. Intriguingly, some of the cells in the ISVZ also displayed radial glia-like morphology without an apical process (Fig. 6*E*), whereas in the human ISVZ these have been hypothesized to be multipolar (Hansen et al. 2010). Taken together, these results proved wrong the possibility that the radial glia-like cells observed in the OSVZ of P1:P3 ferrets could be radial glia cells displaced directly from the VZ. Instead, our results strongly supported the notion that radial glia-like cells in the OSVZ are generated locally from a subpopulation of radial glia-like progenitors undergoing symmetric divisions to self-amplify.

To further confirm the nature of these radial glia-like cells, we labeled them by retrograde infection with *gfp*-encoding adenoviruses. Injection of adeno-*gfp* in the CP of P4 ferrets resulted in the labeling of massive numbers of cells with a process extended radially toward the pial surface and with their soma in the OSVZ, ISVZ, or VZ (Fig. 6*F*). Whereas cells in the VZ displayed an apical process contacting the ventricle, ISVZ and OSVZ cells did not contact the ventricular surface (Fig. 6*F–K*), in agreement with our previous retro-*gfp* labelings. Marker analysis of GFP+ OSVZ cells indicated that 26% of them were Ki67+ progenitor cells, 82% were vimentin+, 98% were Pax6+, and only 2.7% were Tbr2+ (Fig. 6*G–L*). GFP+ cells in the ISVZ had a very similar marker expression profile, where 98% of cells were Pax6+ and only 2.6% were Tbr2+ (Fig. 6*L*). This analysis confirmed that these cells in the OSVZ have radial glia-like characteristics and that many are progenitors. Moreover, their expression of Pax6 but not Tbr2 strongly suggested that these are not neurogenic progenitors (Hevner et al. 2006; Kowalczyk et al. 2009; Hansen et al. 2010), in agreement with our earlier retrovirus analyses indicating these are self-amplifying radial glia-like cells (Fig. 6*A–D*).

Downloaded from https://academic.oup.com/cercor/article/21/7/1674/339599 by guest on 23 April 2024

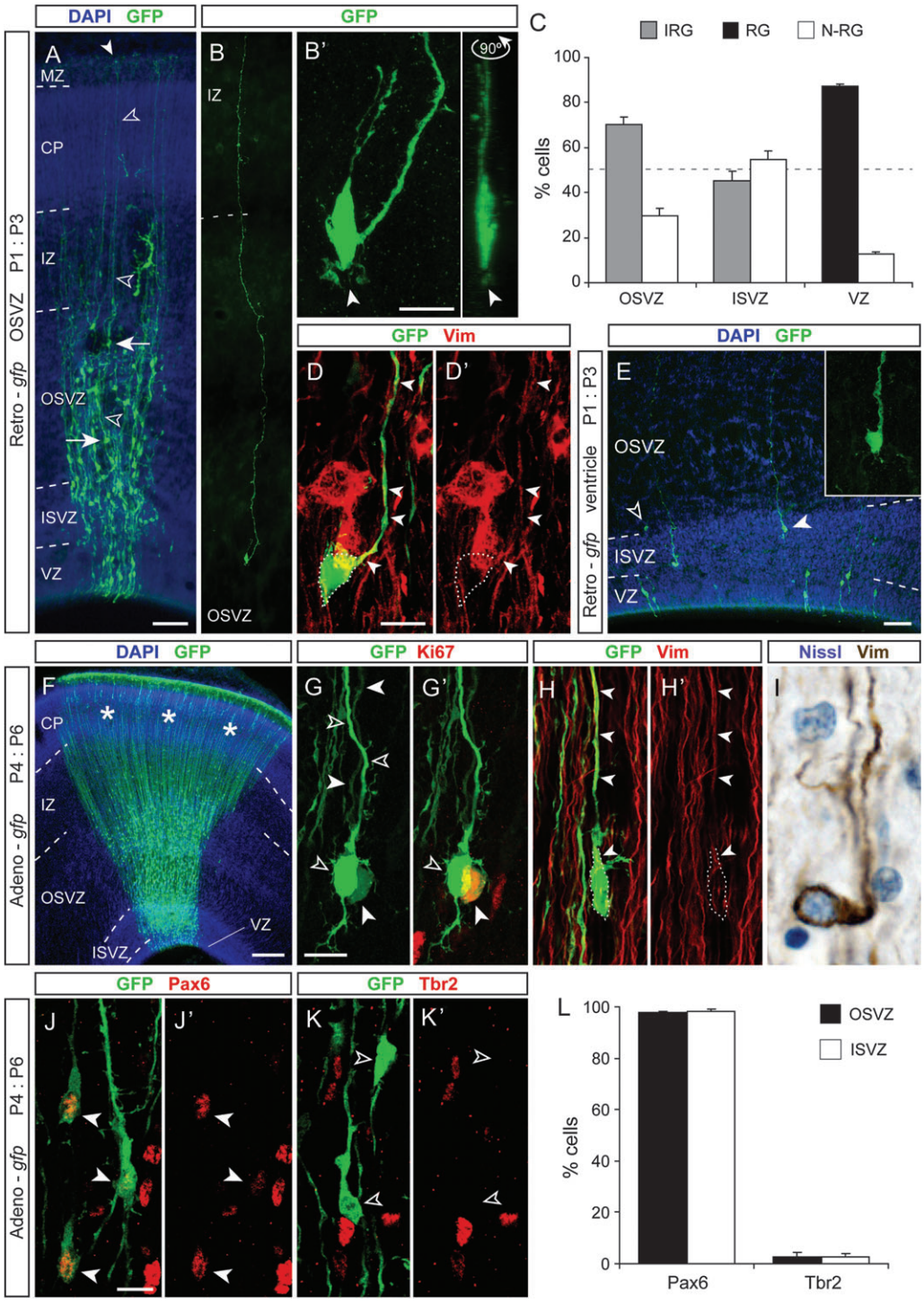

Figure 6. OSVZ progenitors generate IRGCs. (*A–D*) Cells at P3 born in the prospective SG and labeled after injection of retrovirus-*gfp* in the OSVZ at P1. A majority of GFP+ cells display typical radial glia morphology, including an oval soma (arrow) and a radial process (open arrowheads) extended to the surface of the cerebral cortex, branched at the MZ and terminating with end-feet (solid arrowhead in *A*). However, unlike classical radial glia, these IRGCs do not have an apical process contacting the surface of the ventricle. (*B'*) Shows a high magnification confocal image of the cell shown in (*B*), flat and rotated 90°, demonstrating the absence of an apical process in IRGCs. (*C*) Quantification of retrovirus-labeled cells in the specified layers of the prospective SG in P1:P3 animals, indicating proportions of GFP+ cells bearing intermediate radial glia (IRG), classical radial glia (RG), or nonradial glia (N-RG) morphology (mean ± standard error of the mean). Dashed line indicates 50%; $n = 158$ cells (OSVZ), 200 cells (ISVZ), and 125 cells (VZ), 2 animals. (*D*, *D'*) GFP+ cell in the OSVZ with morphology of intermediate radial glia and positive for vimentin (red, arrowheads). (*E*) Labeling of cells at P3 after injection of retrovirus-*gfp* in the telencephalic ventricle at P1. Most GFP+ cells were radial glia in the VZ and multipolar or intermediate radial glia (solid arrowhead) cells in the ISVZ (inset). Only 1 out of 218 GFP+ cells was found in the OSVZ, which was near the border with the ISVZ and had multipolar morphology (open arrowhead). (*F*) Retrograde labeling of cells in the prospective SG at P3 after injection of adenovirus-*gfp* in the CP at P1 (asterisks), including cells in OSVZ, ISVZ, and VZ. (*G–H'*, *J–K'*) OSVZ cells labeled with adeno-*gfp* showing morphology of intermediate radial glia, positive for Ki67 (*G*, *G'*, solid arrowheads), vimentin (*H*, *H'*, arrowheads), Pax6 (*J*, *J'*, arrowheads), and Tbr2 (*K*, *K'*). Open arrowheads in (*G*, *G'*) and in (*K*, *K'*) indicate GFP+ cells negative for Ki67 and Tbr2, respectively. (*I*) Vimentin+ cell in the OSVZ of a human embryo at 16 gestational weeks with morphology typical of intermediate radial glia. (*L*) Proportion of OSVZ and ISVZ cells labeled with adeno-*gfp* positive for the makers indicated (mean ± standard error of the mean). Pax6: $n = 564$ cells OSVZ and 117 cells ISVZ; Tbr2: $n = 283$ cells OSVZ and 205 cells ISVZ; 3 animals. Scale bars—(*A*, *B*): 60 μm; (*B'*, *D–E*, *G–K'*): 10 μm; (*F*): 200 μm.

Downloaded from https://academic.oup.com/cercor/article/21/7/1674/339599 by guest on 23 April 2024

A recent study using slice cultures of embryonic human cerebral cortex has identified a population of radial glia-like progenitors in the OSVZ with morphological traits identical to the cells we have identified here in the ferret OSVZ in vivo, which have been given the generic name of oRG cells (Hansen et al. 2010). However, these progenitors have been shown to be heterogeneous in their mode of division and fate potential: whereas a large subpopulation of progenitors were reported to divide asymmetrically generating 1 neuron and 1 self-renewed progenitor, a second subpopulation divided symmetrically to generate 2 progenitors identical to the mother cell, thus self-amplifying (Hansen et al. 2010). Because this particular subpopulation of self-amplifying OSVZ progenitor cells, only recently described in humans, has not been given a specific name, also because these cells are not radial glia *proper*, and finally because they are very likely to also exist in the human ISVZ (see above), we did not adopt the terminology oRG but named them with the more general term IRGCs. Taken together, our results strongly supported a new model of corticogenesis in gyrencephalic mammals in which, by virtue of generating IRGCs in the OSVZ, new radial fibers are being added to the cerebral cortex during gyrus formation, thus contributing to the fanning of the radial fiber scaffold and therefore, making possible the tangential dispersion of pyramidal neurons and the expansion of the cerebral cortex (Fig. 5*K*).

Binocular Enucleation Reduces OSVZ Proliferation and Cortical Expansion

Next we tested the physiological role of OSVZ progenitor proliferation in cortical expansion. Proliferation of cortical progenitors is known to be modulated by intrinsic and extrinsic influences, of which thalamocortical afferents have been shown to enhance progenitor self-amplification (Dehay et al. 2001; Dehay and Kennedy 2007). In ferret, thalamic axons from the LGN intermingle with OSVZ cells and synapse onto subplate neurons of the developing primary visual cortex (prospective SG) between E28 and P6 (Johnson and Casagrande 1993; Herrmann et al. 1994). Thus, axons from LGN neurons are in the right place at the right time to influence OSVZ progenitor proliferation. Binocular enucleation of neonatal ferrets results in hypoplasia of the LGN (Williams et al. 2002) (Fig. 7*A–C*), so we took advantage of this fact to perturb the thalamic projection from the LGN to the developing visual cortex. First, we examined if binocular enucleation at P1 affected the proliferation of progenitors in the prospective visual cortex. We found that 1 day after enucleation (P2) the density of PH3+ cells in the OSVZ of A17 was 15% lower in enucleated animals compared with controls ($P < 0.05$, $n = 4$ sections per animal, 3–4 animals per group; Fig. 7*D–F*). This effect appeared to be quite specific for this layer and age as statistically significant differences were not detected in the OSVZ at later stages and never in the ISVZ or VZ (Fig. 7*F* and Supplementary Fig. S9). Density of proliferation was also indistinguishable between enucleated and control animals in A19 throughout the layers and at all ages examined (Supplementary Fig. S9). Therefore, binocular enucleation at P1 systematically resulted in reduction of OSVZ proliferation in A17 at P2, which was precisely the age when we had observed self-amplification of IRGCs (Fig. 6*C*).

Next we studied which types of progenitors were underproliferating in the OSVZ of enucleated animals at P2. Our previous marker analyses demonstrated that the vast majority of ferret OSVZ progenitors express Pax6, whereas only a subpopulation express Tbr2, which is observed in putative neurogenic progenitors (Kowalczyk et al. 2009; Hansen et al. 2010). PH3–Tbr2 double-staining analyses in the OSVZ revealed that in enucleated animals the density of Tbr2–/PH3+ cells (nonneurogenic) was 34% lower than in controls, whereas the density of Tbr2+/PH3+ progenitors (neurogenic) was not changed (Fig. 7*G*). In contrast, analyses of ISVZ and VZ revealed no changes in the proportion of either of these 2 types of progenitors upon enucleation. Taken together, these findings indicated that binocular enucleation did not affect neurogenesis but specifically impaired the proliferation of Tbr2-negative progenitors in the OSVZ and hence diminished the generation of putative IRGCs.

According to our hypothesis, a decrease in the generation of IRGCs would reduce the tangential expansion of the cerebral cortex. In agreement with this hypothesis, when enucleated ferrets were allowed to develop to maturity (P48), we found that the perimeter of the SG was 23% smaller than in control animals (Fig. 7*H–J* and Supplementary Fig. S10). Changes in the size or shape of cortical folds may occur, however, without a reduction in cortical surface area but simply due to changes in the deformation of the cortical sheet. If this was the case in enucleated ferrets, we would expect that the absolute size of visual area A17 would not change significantly, but only the location of its borders. We found that the location of A17 borders in enucleated animals was the same as in controls, but this cortical area was dramatically smaller in perimeter. By using a variety of markers that delimit A17 in control animals, including acetyl cholinesterase stain (Rockland 1985) and expression of *cdh8*, *cdh20*, and *pcdh10* mRNA (Krishna et al. 2008), we found that A17 was 35–40% smaller in enucleates than in controls (Fig. 7*J–N* and Supplementary Figs S11 and S12).

Such dramatic reduction in the size of this cortical area could also be attributed to increased cell death of cortical neurons. We tested for cell death in the prospective SG by detection of activated caspase 3 and found minimal numbers of labeled cells in the postmitotic layers (CP, IZ, and OSVZ), with no statistically significant differences between control and enucleated animals (Supplementary Fig. S13). Altogether, our results demonstrated that reduced proliferation of Tbr2-negative OSVZ progenitors, but not reduced neurogenesis or increased cell death, led to the formation of a smaller A17 in enucleated animals and, hence, a smaller SG.

Reduced OSVZ Proliferation Impairs the Tangential Dispersion of Cortical Neurons

Enucleated animals suffered a decrease in OSVZ proliferation generating IRGCs but not in neurogenic proliferation in OSVZ, ISVZ, or VZ. If normal numbers of neurons were made, but the surface area of the SG was smaller, we hypothesized that cortical neurons should pile up in thicker layers as it has been shown to occur in human lissencephaly and pachygyria (Walsh 1999; Hong et al. 2000). Measurement of Nissl-stained sections demonstrated that at the SG the cortex was 12% thicker in enucleates than in controls (controls, 983 ± 22.5 μm; enucleates, 1102 ± 22.5 μm; $P < 0.01$, $n = 3–7$ animals per group). When examined individually, however, only layers 5 and 6 increased in thickness but not layers 2/3 or 4 (Fig. 8*A–C*). Staining with layer-specific markers (Molyneaux et al. 2007)

Downloaded from https://academic.oup.com/cercor/article/21/7/1674/339599 by guest on 23 April 2024

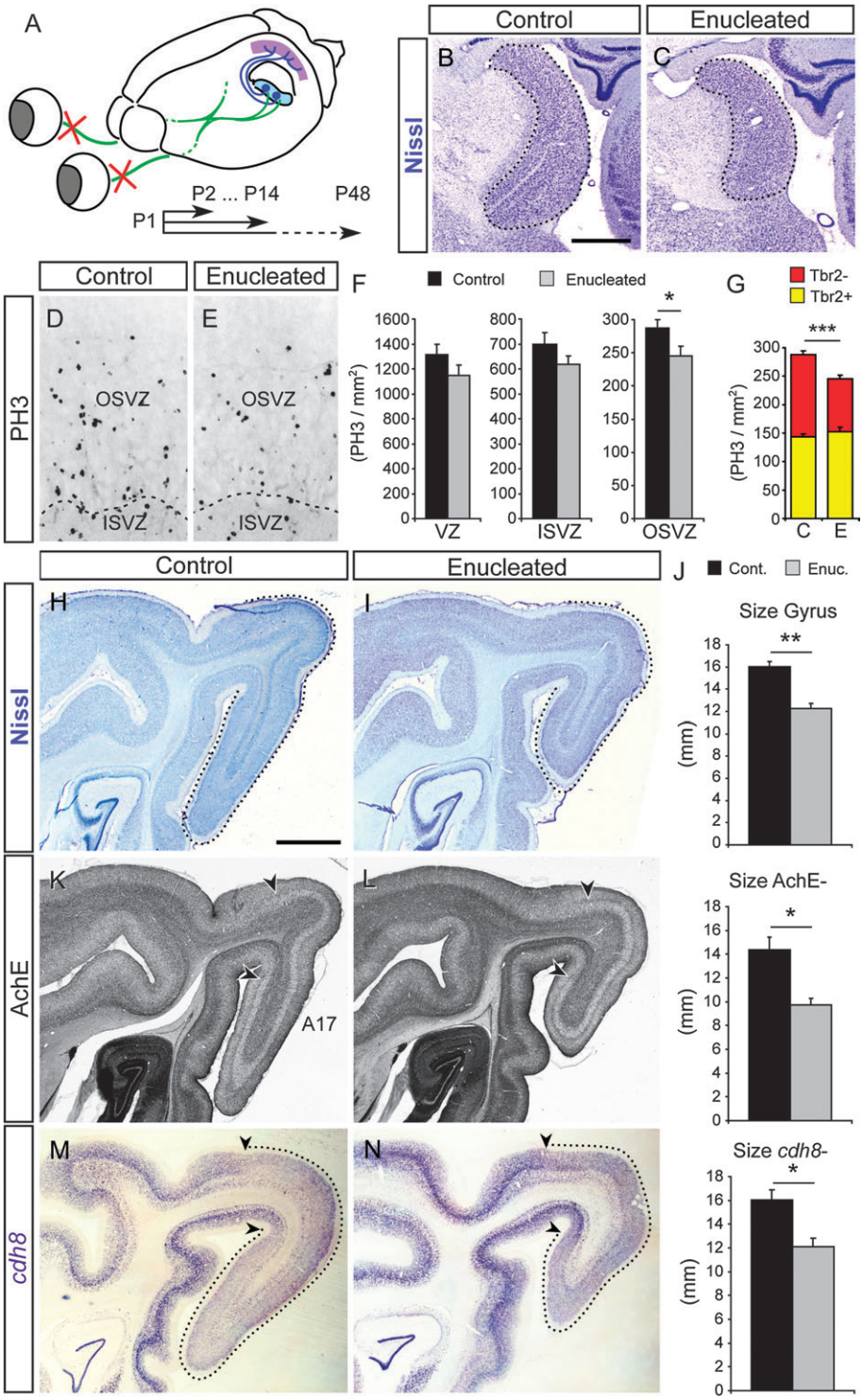

Figure 7. Effects of binocular enucleation on OSVZ proliferation and cortical expansion. (*A*) Schematic of the experimental design. Binocular enucleation at P1 results in degeneration of retinal axons (green) projecting to the LGN (blue), which itself projects to the primary visual cortex (purple). Animals were analyzed at various postnatal ages. (*B*, *C*) Nissl stains of sagital sections at the level of the LGN (dotted contours) from control and enucleated ferrets at P48. (*D–F*) Immunodetection of PH3 in the prospective A17 of control and enucleated ferrets at P2 (*D*, *E*) and quantification of the density of PH3+ cells in the OSVZ, ISVZ, and VZ in P2 animals (*F*). (*G*) Density of PH3+ cells in the OSVZ of P2 control (*C*) and enucleated (*E*) animals which are positive or negative for Tbr2. (*H–N*) Patterns of stain of Nissl substance (*H*, *I*), acetyl cholinesterase (*K*, *L*), and *cdh8* mRNA (*M*, *N*) in the occipital cortex of control and enucleated ferrets at P48, and quantifications of the perimeter of the cortical area identified with each of these stains (*J*). The extent of identified areas is indicated by dotted lines, and arrowheads indicate the borders with neighboring areas. Images and quantifications are from sections at an approximate level of 7.5 mm from the lateral border of the brain; $n = 2$–4 animals per group. Enucleation caused a dramatic decrease in the size of the SG, which was caused by a significant reduction in the size of A17. $^{*}P < 0.05$, $^{**}P < 0.01$, $^{***}P < 0.0001$, *t*-test. Scale bars—(*B*, *C*): 1 mm; (*D*, *E*): 100 μm; (*H–N*): 2 mm.

Downloaded from https://academic.oup.com/cercor/article/21/7/1674/339599 by guest on 23 April 2024

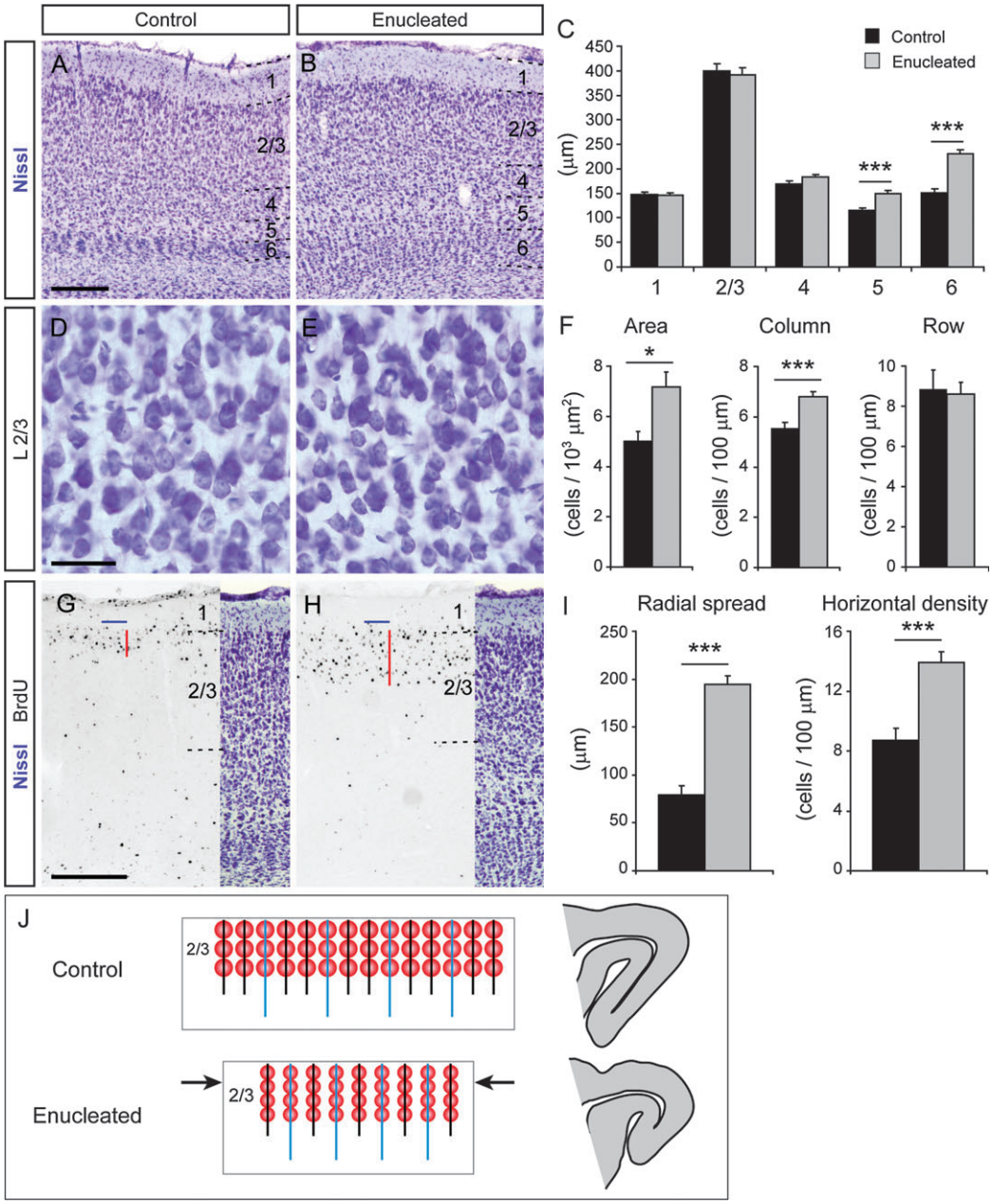

Figure 8. Effects of binocular enucleation on the laminar organization of the SG. (*A–F*) Nissl-stained sections of the SG at equivalent levels in control and enucleated ferrets illustrating differences in the thickness of cortical layers (*A*, *B*) and size and density of neurons within layer 2/3 (*D*, *E*). (*C*) Quantification of the thickness of individual cortical layers in control and enucleated ferrets ($n = 4$ controls, 7 enucleated). (*F*) Quantification within layer 2/3 of cell density across the layer ($n = 691$ cells in 8 fields, controls; 1,452 cells in 14 fields, enucleated), cell density along a vertical column ($n = 514$ cells in 32 columns, controls; 967 cells in 56 columns, enucleated), and cell density along a horizontal row ($n = 86$ cells in 16 rows, controls; 140 cells in 28 rows, enucleated). Images and quantifications are all from sections 7.5 mm from the lateral border of the brain. In enucleated animals, layer 2/3 was similar in thickness, but it contained a higher density of cells across the layer, and per column, than controls. (*G*, *H*) BrdU stains of sections from A17 of control and enucleated ferrets at P48 after BrdU administration at P1, and Nissl stains of adjacent sections to define layer borders. (*I*) Quantification of the vertical spread of BrdU+ cells, as indicated by red bars in (*G*, *H*) and of the number of BrdU+ cells under a 100-μm horizontal strip of cortex, as indicated by blue bars in (*G*, *H*); $n = 424$ cells, 8 fields, 2 animals, control, and 998 cells, 12 fields, 3 animals, Enucleated. (*J*) Schematic illustrating differences observed in composition and organization of layer 2/3 between control and enucleated ferrets. In enucleated animals, the horizontal density of cells (spacing between cell columns) is normal; however, because there are more cells per column, the total population of cells accumulates in a smaller surface area of cortex (horizontal arrows), resulting in a smaller gyrus. However, because cells are smaller in enucleates, layer thickness does not increase. $^*P < 0.05$, $^{***}P < 0.001$, *t*-test. Scale bars—(*A*, *B*): 300 μm; (*D*, *E*): 50 μm; (*G*, *H*): 300 μm.

demonstrated that the lack of thickening in layers 2/3 and 4 was not due to mispositioning of cells from these to lower layers (Supplementary Fig. S14). Because neurons destined for layer 2/3 were still migrating at the time of enucleation (Jackson et al. 1989), we had expected that this layer would be the most affected by the reduction in IRGCs. Further analyses showed that, in part, layer 2/3 had not increased in thickness because in enucleated ferrets the density of cell somas was higher (Fig. 8*D–F*), and these were smaller than in control animals (controls, 131.6 ± 1.8 μm^2; enucleates, 106.3 ± 1.0 μm^2; $P < 10^{-5}$; $n = 676$ cells, 3 animals in controls; $n = 1{,}314$ cells, 7 animals in enucleates). More specifically, the greater cell

Downloaded from https://academic.oup.com/cercor/article/21/7/1674/339599 by guest on 23 April 2024

density in layer 2/3 was due to increased density of cells per cortical column, along the vertical axis, but not in the density of cells along cortical rows (Fig. 8*D–F*). These results demonstrated that in enucleated ferrets, cortical columns were fewer than in control animals but contained larger numbers of layer 2/3 cells, further supporting the notion that the tangential dispersion of radially migrating neurons had been compromised (Fig. 8*J*). This was confirmed by BrdU-labeling experiments, which showed that in layer 2/3 of enucleated ferrets cortical columns contained a larger number of late-born cells than in control animals (Fig. 8*G–I*).

Discussion

In the present study, we provide compelling evidence that the tangential expansion of the cerebral cortex relies on the proliferation of OSVZ progenitors, which undertake previously unsuspected functions. First, we demonstrate that OSVZ progenitors are not unique to primates but are also present in all gyrencephalic mammals examined. Next we show that patterned differences in VZ and ISVZ proliferation across regions of the embryonic cerebral cortex lead to differences in neuron production, and these are coupled to parallel variations in proliferation at the OSVZ. OSVZ progenitors are responsible for generating IRGCs, a population of self-amplifying progenitors with particular morphological characteristics that specifically contribute to the divergence of the radial fiber scaffold, which in turn drives the tangential dispersion of radially migrating neurons and, finally, the expansion in surface area of the cerebral cortex (Fig. 9).

Cellular Substrates for Cortical Expansion: IRGCs

By comparison with lissencephalic species, it is clear that the development of convoluted brains requires two coordinated events: 1) the production of greater numbers of cortical

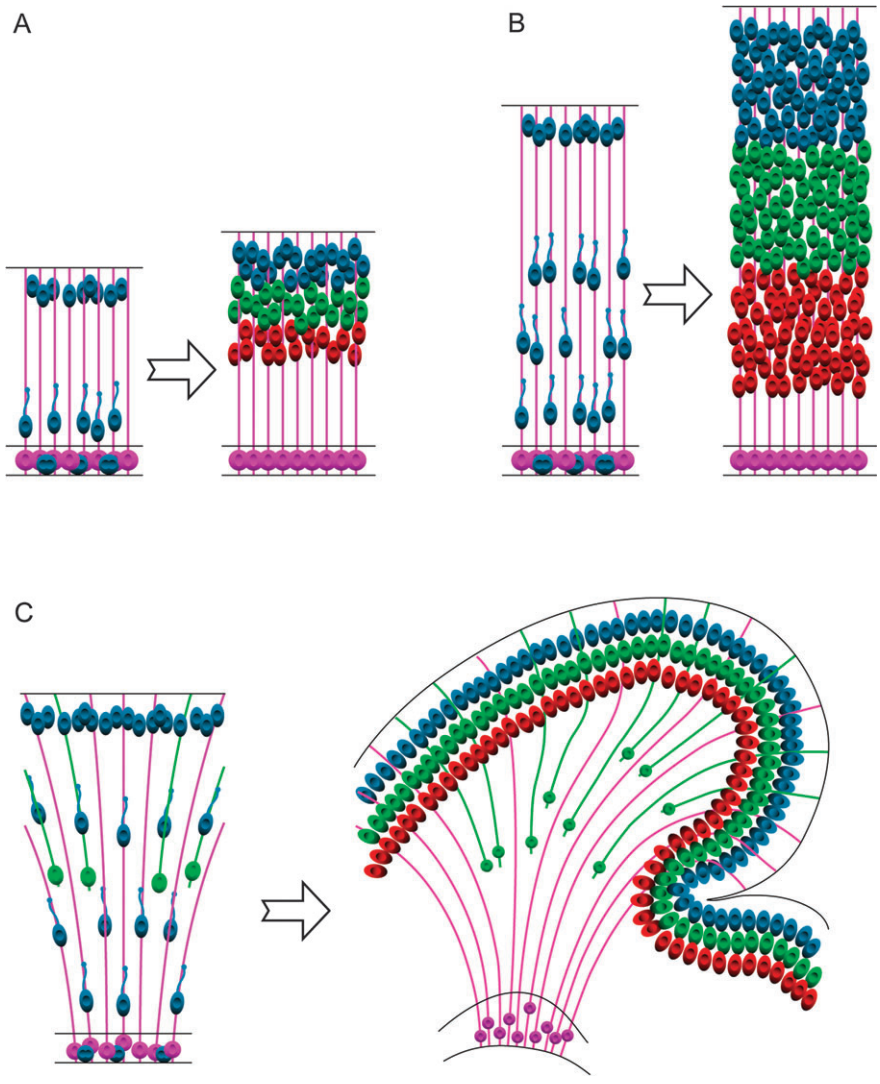

Figure 9. Mechanisms for tangential versus radial expansion of the cerebral cortex. (*A*) In species with a smooth cortex, like mouse, radial fibers are mostly parallel (pink) and migrating neurons follow those same parallel trajectories (blue), resulting in virtually no tangential dispersion with respect to the positions of their progenitor cells in the VZ (pink and blue circles). (*B*, *C*) In species with convoluted brains, like carnivores and primates, including human, the radial fiber scaffold may display 2 conformations: parallel or divergent. If radial fibers are parallel (*B*), neurons generated by cortical progenitors will accumulate on thick layers (red, green and blue) without much tangential dispersion. But if radial fibers are divergent (*C*), cortical neurons will migrate following divergent trajectories and will disperse tangentially, thus increasing the final surface area and degree of convolution of the cerebral cortex. In this second model, radial fibers from IRG (green) intercalate between full-span fibers of classical radial glia cells (pink).

Downloaded from https://academic.oup.com/cercor/article/21/7/1674/339599 by guest on 23 April 2024

neurons and 2) the tangential dispersion of migrating neurons, so that a larger cortical surface area is generated instead of a thicker cortex (Fig. 9). Regarding neurogenesis, here we show that in gyrated brains the rate of proliferation of neurogenic progenitors is heterogeneous along the cortex, being much more abundant in cortical regions undergoing the greatest expansion. A similar situation has been shown in the macaque, where marked differences in progenitor cell cycle dynamics determine striking cytoarchitectural differences between cortical areas (Dehay et al. 1993; Lukaszewicz et al. 2005). This occurs much less dramatically during the development of the smooth rodent cortex (Bayer and Altman 1991; Polleux, Dehay, and Kennedy 1997; Polleux, Dehay, Moraillon, and Kennedy 1997), further suggesting that it may be a strategy particularly beneficial for gyrencephaly.

Regarding the tangential dispersion of migrating neurons, this may seem to suggest the movement of cortical neurons along the tangential axis, parallel to the cortical surface. However, only cortical interneurons migrate tangentially for long distances in a manner independent of radial glia (Marin and Rubenstein 2001), whereas the radial migration of cortical excitatory neurons is known to be strictly dependent on radial glia fibers, which span perpendicular to the cortical surface (Rakic 1972; Sidman and Rakic 1973; Schmechel and Rakic 1979a; Misson et al. 1991; Anton et al. 1997; reviewed in Marin and Rubenstein 2003). Then how can migrating pyramidal cells, which depend on radial glia, disperse tangentially in a direction orthogonal to that of radial glia fibers? Pioneer studies of radial glia in the macaque cerebral cortex showed that parallel radial fibers follow curved trajectories accommodating to the incipient folding of the cerebral cortex (Schmechel and Rakic 1979a), but this is insufficient to explain the tangential dispersion of radially migrating cells. Instead, here we describe the existence of a specific type of progenitor, IRGC, which provides a structural explanation for how migrating excitatory neurons that depend on radial glia fibers can still do so and at the same time they can disperse tangentially, without the need for a true tangential migration (Fig. 9).

Classical studies using Golgi staining and inmunohistochemical methods, and recent analyses using time-lapse analysis, have identified cells with morphology very similar to IRGCs in the developing cerebral cortex of various gyrencephalic and lissencephalic species, including rabbit, rat, ferret, macaque, and human (Ramon y Cajal 1891; Rakic 1972; Sidman and Rakic 1973; Choi and Lapham 1978; Schmechel and Rakic 1979a; Voigt 1989; deAzevedo et al. 2003; Noctor et al. 2004; reviewed in Rakic 2003a, 2003b). These cells were named "displaced radial glial cells" and simply interpreted as being astrocytic progenitors or cells on their way to transforming into astrocytes, although their relative abundance in different species and their potential to transiently influence the radial migration of cortical neurons were never examined in depth. Alternative to those early interpretations, a recent study using clonal analysis has shown that cells with this same morphology found in the human OSVZ during midgestation are primarily neurogenic progenitors and have been named oRG (Hansen et al. 2010). In addition to neurogenesis, it has been shown that there is a subpopulation of oRG cells with the potential to self-amplify, producing 2 oRGs out of each cell division (equivalent to the ferret cells we have named IRGCs), although this is suggested to occur rarely. oRGs have been proposed to be specific to the OSVZ and to be unique to humans (Hansen et al. 2010). In contrast, our present findings show for the first time that 1) IRGCs are not unique to humans or even primates, but rather they are also abundantly present in other gyrencephalic species like the ferret; 2) ferret IRGCs self-amplify much more often than initially reported in human (Hansen et al. 2010); 3) IRGCs are directly involved in the histogenetic process of cortical expansion and folding by expanding the scaffold of radial glia fibers in a fanned array; and 4) the final fate of IRGCs is to become astrocytic progenitors or cells on their way to transforming into astrocytes, as revealed by our long-term retroviral lineage analysis of OSVZ progenitors (Fig. 4). This is consistent with pioneer studies of "displaced radial glial cells" in ferret, macaque, and human (Rakic 1972; Sidman and Rakic 1973; Choi and Lapham 1978; Schmechel and Rakic 1979a; Voigt 1989; deAzevedo et al. 2003), and is also consistent with our unpublished observations that in the ferret cerebral cortex GFAP+ astrocytes are only visible in OSVZ or IZ after P6, well after the period of self-amplification of IRGCs.

Tbr2 expression appears to be a general feature of neurogenic progenitors, both in rodents and in humans (Kowalczyk et al. 2009; Hansen et al. 2010). However, whereas in the rodent SVZ neurogenic intermediate progenitor cells (IPCs) are multipolar, contacting neither the ventricular nor the pial surface, neurogenic progenitors in the human OSVZ (oRG) are highly polarized cells retaining many features typical of radial glia cells, including contact with the pial surface (Noctor et al. 2004; Hansen et al. 2010). In ferret, on the other hand, we find an intermediate situation: the OSVZ contains IRGCs morphologically similar to human oRG, but these do not express Tbr2 nor contribute very significantly to cortical neurogenesis. Given that ferret VZ progenitors generate multipolar cells and that the majority of cortical neurons in the ferret derive from these progenitors, it is tempting to speculate that the ferret also contains neurogenic IPCs similar to those in mouse. Are there transitional forms between IRGCs and IPCs? IPCs are characterized by multipolar morphology and Tbr2 expression, following quick downregulation of Pax6 (Hevner et al. 2006), whereas our analyses indicate that in the ferret a very small proportion of IRGCs express Tbr2 and the majority express Pax6. However, we have also found that about 45% of OSVZ progenitors coexpress Pax6 and Tbr2. This suggests the potential existence of numerous progenitors in transition between IRGCs and IPCs at the level of transcription factor expression but with morphology different from IRGCs.

A recent report proposed that the ferret SVZ contains 2 classes of progenitors: type ISVZ and type OSVZ (Fietz et al. 2010). However, the distinction between ISVZ and OSVZ was not based on cytoarchitectonic and proliferative differences (as all germinal layers are defined [Boulder Committee 1970; Smart et al. 2002; Lukaszewicz et al. 2005; Bystron et al. 2008]) but instead based on cell morphology and gene expression, where Pax6 would define OSVZ progenitors and Tbr2 would define ISVZ progenitors. Our detailed analysis challenges this simplistic view by demonstrating that ferret progenitors are quite heterogeneous in OSVZ and ISVZ, with Pax6+, Tbr2+, and Olig2+ progenitors coexisting extensively in both layers. Moreover, we demonstrate that ISVZ and OSVZ exist, as anatomically distinct germinal layers, in a variety of nonprimate species (Figs. 1*A* and 2*A*).

In humans, it has been proposed that the OSVZ is simply a duplicated neurogenic layer containing the same progenitor types and in the same proportions as the VZ–ISVZ

Downloaded from https://academic.oup.com/cercor/article/21/7/1674/339599 by guest on 23 April 2024

(Hansen et al. 2010). Unfortunately, in that study the ISVZ was not distinguished from the VZ, whereas our detailed analysis reveals that in ferret the VZ is much different than the ISVZ. This suggests the possibility that also human ISVZ and VZ may be different from each other and that each of the 3 main germinal layers may serve particular and specialized roles in cortical development. Although it is unlikely that the extraordinary diversity of progenitor cells found in the human OSVZ is paralleled in species with a less complex cerebral cortex (Zecevic et al. 2005; Howard et al. 2006; Hansen et al. 2010), our characterization demonstrated that the population of OSVZ progenitors in the ferret is considerably heterogeneous and complex, that it shares many similarities with the human OSVZ at the molecular level, and that it is quite different from the population of progenitors in the mouse SVZ.

Control of Cortical Size

Our loss-of-function experiments performing binocular enucleation in ferret illustrate that cortical expansion is not an all-or-none process, but it can be finely modulated by modifying the proliferation of OSVZ progenitors. Our present analyses reveal that the immediate effect of binocular enucleation on the developing cerebral cortex of the ferret is to reduce the proliferation of Tbr2-negative OSVZ progenitors in A17, which are responsible for the local generation of IRGCs, but not that of Tbr2+ OSVZ progenitors, ISVZ, or VZ progenitors, which we have shown to be primarily neurogenic. These findings explain the reduction in surface area of A17 in enucleated ferrets and also that the numbers of cortical neurons appear to remain largely unchanged. Binocular enucleation had been performed previously in macaque monkeys as an experimental paradigm to investigate the influence of thalamic afferents over cortical development (Rakic 1988; Dehay et al. 1996a, 1996b). Those pioneer studies concluded that, in macaques, enucleation leads to a reduction of the striate visual cortex (primary visual cortex in primates), which becomes partly respecified into additional extrastriate visual cortex, and so the overall size in surface area of the neocortex remains unchanged (Dehay et al. 1996a). Interestingly, our current findings demonstrate that, in the ferret, the long-term consequences of binocular enucleation are also a dramatic reduction in the size of the primary visual cortex (area 17), but in this case, there is no respecification or enlargement of neighboring areas, and so the surface area of the cerebral cortex is effectively reduced. Why are the long-term effects of binocular enucleation so different between macaque and ferret? Answering this question requires analyzing the early effects of binocular enucleation on the developing cerebral cortex of macaque embryos, which unfortunately has never been done.

One of the most relevant conclusions of our binocular enucleation experiments is that neuron production and cortical expansion–folding are 2 mechanisms largely dissociable. In the ferret, cortical neurons are mostly born from VZ–ISVZ progenitors, whereas IRGCs are born in the OSVZ. Similarly, whereas thalamocortical afferents appear to influence OSVZ proliferation, they seem to exert little influence over VZ–ISVZ progenitors in the ferret. Our experiments further demonstrate that reducing proliferation in the OSVZ but not in the neurogenic progenitors leads to abnormal thickening of the cortical layers, which indicates that the processes of neurogenesis and of tangential expansion must be coordinated with great precision in the developing cerebral cortex. This notion is consistent with evidence from human neuropathology. Human lissencephaly is characterized by reduced tangential growth of the cerebral cortex and a partial or complete absence of cortical folds (Walsh 1999; Ross and Walsh 2001). Among the heterogeneous group of lissencephalic malformations, pachygyria is characterized by the formation of abnormal folds that are both reduced in number and unusually thick. As a result, the cerebral cortex is significantly smaller in surface area but not obviously reduced in neuronal numbers (Walsh 1999). In contrast to pachygyria, individuals suffering from microcephaly show a substantial reduction in size of the cerebral cortex but exhibit normal neuronal migration and architecture, including folds and fissures with a remarkably normal appearance (Bond et al. 2002), which suggests deficient neurogenesis but proportionally normal tangential expansion. Taken together, these observations support the notion that cortical neurogenesis and tangential expansion may be 2 processes mechanistically dissociable and suggest that selective reductions in OSVZ proliferation may contribute to human cortical malformations such as pachygyria, although further research is needed to test these hypotheses.

How are neurogenesis and tangential dispersion orchestrated during development? Although much is known about the intracellular mechanisms regulating neurogenesis and cell cycle progression in the cerebral cortex (reviewed in Dehay and Kennedy 2007), little is known about the non–cell-autonomous regulation of OSVZ progenitors (Lukaszewicz et al. 2005). Our experiments of binocular enucleation suggest that thalamic afferents may play an important modulatory influence over OSVZ progenitors in vivo as it has been previously shown in vitro for rodent VZ progenitors (Gong and Shipley 1995; Dehay et al. 2001). This could be mediated through the secretion of growth factors by thalamic axons onto OSVZ cells (Dehay et al. 2001). Although much work needs to be done in this direction, binocular enucleation in ferret may proof to be a good paradigm to search for molecules controlling OSVZ progenitor dynamics and fate.

Control of Cortical Shape

The tangential expansion and stereotypic folding of the cerebral cortex as observed in large mammals is a complex process likely involving many different developmental events and genetic networks (Welker 1990; Ross and Walsh 2001; Piao et al. 2004; Rakic 2004). The patterns of folds and fissures are largely preserved between individuals of any given species, including rather complex patterns like in the human cortex, which suggests a strong genetic basis (Welker 1990; Lohmann et al. 1999; Rakic 2004; Lohmann et al. 2007). However, a precise control over neurogenesis and radial fiber divergence alone is likely to be insufficient to systematically attain these complex patterns of convolution. A plausible alternative is that after neural progenitors and radial glia establish a basic pattern of differential cortical growth, other factors take part in shaping and folding the cortical sheet in more exquisite patterns (Neal et al. 2007). Tension forces and hydraulic pressures have been proposed as strong candidates (Caviness 1975; Van Essen 1997; Toro and Burnod 2005; Hilgetag and Barbas 2006). Indeed, while also having a genetic basis, these mechanical forces may be able to act more locally and precisely than earlier mechanisms and may thus play a more direct role in determining the specific shapes of distinct cortical folds and fissures. We should learn from future studies how all these

Downloaded from https://academic.oup.com/cercor/article/21/7/1674/339599 by guest on 23 April 2024

mechanisms are finely regulated and orchestrated, so that the end product is an expanded, but coherent and functional, cerebral cortex (Rajimehr and Tootell 2009).

IRGCs and Current Hypotheses of Neocortical Expansion during Evolution

The "radial unit hypothesis" states that the surface area of the cerebral cortex is determined by the size of the neuroepithelial progenitor pool in the VZ at the onset of neurogenesis and that a bigger or smaller size of this germinal layer is expected to increase or decrease the surface area of the mature cerebral cortex (Rakic 1995a). It also postulates that the thickness of the cerebral cortex depends on the neuronal output of each progenitor cell, which may depend on a number of factors including the length of the neurogenetic period and the number of neurogenetic cell cycles (Rakic 1995a). Our results add a second dimension to this radial hypothesis and show that surface area of the cerebral cortex also depends critically on the tangential expansion of the radial fiber scaffold. Our model proposes that in gyrencephalic species, as a result of the generation of IRGCs and the subsequent divergence of the radial fiber scaffold, the neurons generated from each individual cortical progenitor disperse tangentially and form, not just one, but multiple cortical columns. In agreement with the radial unit hypothesis, our present findings in ferret, cat, and human demonstrate that the density of progenitor divisions is greater in areas with greater cortical growth. However, because in these areas IRGCs are particularly abundant and the radial fiber scaffold is expanded, such increased neurogenesis does not translate into a thicker cerebral cortex but into a larger surface area. Finally, since the expanded radial fiber scaffold of gyrencephalic species still retains the positional information of neurogenic progenitors in the VZ (Fig. 5), a cortical protomap potentially existing in the neuroepithelial progenitor layer would still be efficiently translated to the emerging neuronal layers of the cerebral cortex (Rakic 1988; O'Leary and Borngasser 2006).

Phylogenic Conservation of Developmental Mechanisms Driving Cortical Folding

How did IRGCs originate during mammalian phylogeny? Multiple lines of evidence suggest that cortical progenitors, and in particular radial glia cells, have evolved significantly over the last 90 million years since primate and rodent phylogeny separated (Bininda-Emonds et al. 2007). Several morphological and molecular features of cortical progenitors and radial glia cells are significantly different between mouse, ferret, macaque monkey, and human (Rakic 1972, 2003b; Sidman and Rakic 1973; Schmechel and Rakic 1979a; Takahashi et al. 1990; Gadisseux et al. 1992; deAzevedo et al. 2003). First, in carnivores and higher primates radial fibers adopt curved trajectories and can reach up to 3–7 mm in length, as opposed to the straight course of the short mouse radial glia fibers (Rakic 1972, 2003b; Takahashi et al. 1990; Gadisseux et al. 1992). Second, detached radial glia cells in the human OSVZ (oRG) and IRGC are progenitor cells self-amplifying, self-renewing, or generating neurons, whereas detached radial glia in the mouse only produce, or transform into, astrocytes (Takahashi et al. 1990; Noctor et al. 2001; Hansen et al. 2010). Third, progenitors in the ferret, macaque, and human OSVZ are highly heterogeneous and express a variety of combinations of different transcription factors including Pax6, Tbr2, Sox2, and Olig2, whereas in the mouse SVZ virtually all progenitors express Tbr2 and not Pax6 (Englund et al. 2005; Zecevic et al. 2005; Howard et al. 2006; Mo et al. 2007; Mo and Zecevic 2008; Hansen et al. 2010). Fourth, in human and macaque, numerous radial glia cells detached from the ventricular surface remain with their soma in the OSVZ and IZ for long periods of time, while elaborating many short processes along their radial fiber (Rakic 1972, 2003b; Sidman and Rakic 1973; Schmechel and Rakic 1979a; deAzevedo et al. 2003). Fifth, radial glia cells in primates express the intermediate filament GFAP, whereas in mouse and carnivores they only start expressing GFAP when transforming into astrocytes (Choi and Lapham 1978; Schmechel and Rakic 1979b; Levitt and Rakic 1980; Voigt 1989; Rakic 1995a, 2003b). Finally, the SVZ of the human cerebral cortex is the largest, lasts for longer, and appears proportionately earlier than in other mammals (Zecevic et al. 2005; Bystron et al. 2008). All these observations, together with our present findings, support the notion that the transient population of radial glia cells has evolved significantly and in parallel to the expansion and folding of the cerebral cortex during mammalian phylogeny.

Until now, the OSVZ was hypothesized to play important roles in cortical expansion and complexity, but it was thought to be present only in primates. However, gyrencephaly is found not only in primates but also in species of all major families of mammals, including rodents (the closest relatives to primates), carnivores, ungulates, and even in species as far apart in evolution as marsupials and monotremes (http://www.brain-museum.org) (Bininda-Emonds et al. 2007). Here we describe the existence of a germinal layer similar to the primate OSVZ in the developing cerebral cortex of multiple gyrencephalic species belonging to various mammalian orders (Smart et al. 2002; Zecevic et al. 2005; Bayatti et al. 2008). We also demonstrate that the proportion of cortical progenitors found in the OSVZ of any given species is highly correlated with its degree of cortical convolution. This correlation strongly supports 2 concepts: 1) the OSVZ is central for cortical folding (Smart et al. 2002; Zecevic et al. 2005; Kriegstein et al. 2006; Dehay and Kennedy 2007; Bystron et al. 2008) and 2) the basic developmental mechanisms involved in cortical folding are likely conserved across mammalian phylogeny. Because these developmental mechanisms are likely to be quite complex, including the generation of IRGCs and the existence of a very heterogeneous population of OSVZ progenitors, it is unlikely that these mechanisms appeared independently and multiple times during mammalian evolution. Instead of invoking evolutionary convergence, we propose that OSVZ progenitors and IRGCs might have already been present in the ancestor common to all extant mammals, existing about 160 million years ago (Bininda-Emonds et al. 2007) and that such ancestor probably also displayed some degree of gyrencephaly. This would imply a secondary loss of OSVZ progenitors and IRGCs in lissencephalic mammals. Our current findings provide a plausible explanation for the evolution of developmental mechanisms involved in the expansion and folding of the mammalian cerebral cortex.

Supplementary Material

Supplementary Figures S1–S14 and Tables S1 and S2 can be found at: http://www.cercor.oxfordjournals.org/

Downloaded from https://academic.oup.com/cercor/article/21/7/1674/339599 by guest on 23 April 2024

Funding

International Human Frontier Science Program Organization, Spanish Ministry of Science and Innovation (MICINN) (grant numbers BFU2006-08961/BFI, SAF2009-07367); Consejo Superior de Investigaciones Científicas (grant number 200820I027); Generalitat Valenciana (grant number GV/2007/054); CONSOLIDER (grant number CSD2007-00023 to V.B.); MICINN (FPU predoctoral fellowship to I.R. and "Juan de la Cierva" postdoctoral fellowship to C.d.J.R.).

Notes

We are indebted to E. M. Callaway for his extremely generous support during the initial stages of this project. We thank the Department of Pathology of the Hospital Universitario La Paz in Madrid, in particular to Dr J. I. Rodriguez and Dr C. Morales, for their support and for giving us access to human fetal brain tissue from their necropsy procedures, and P. Rubio for expert technical assistance in processing human tissue samples; J. I. Johnson for providing the adult human brain image shown in Figure S5; F. H. Gage for generously providing retrovirus-*gfp* stocks; C. Redies and O. Marin for cDNA probes; S. Chatterjee and E. Tan for programming; M. de la Parra and S. Tye for assistance during surgeries; and M. Bonete and M. Luna for technical help. We also thank C. Garcia-Frigola, N. Flames, M. Valiente, B. Rico, O. Marin, and M. A. Nieto for discussions and critical reading of the manuscript. *Conflict of Interest* : None declared.

References

Anton ES, Marchionni MA, Lee KF, Rakic P. 1997. Role of GGF/neuregulin signaling in interactions between migrating neurons and radial glia in the developing cerebral cortex. Development. 124:3501–3510.

Armstrong E, Schleicher A, Omran H, Curtis M, Zilles K. 1995. The ontogeny of human gyrification. Cereb Cortex. 5:56–63.

Bayatti N, Moss JA, Sun L, Ambrose P, Ward JF, Lindsay S, Clowry GJ. 2008. A molecular neuroanatomical study of the developing human neocortex from 8 to 17 postconceptional weeks revealing the early differentiation of the subplate and subventricular zone. Cereb Cortex. 18:1536–1548.

Bayer SA, Altman J. 1991. Neocortical development. New York: Raven Press.

Bayer SA, Altman J. 2005. The human brain during the second trimester. New York: CRC Press.

Bininda-Emonds OR, Cardillo M, Jones KE, MacPhee RD, Beck RM, Grenyer R, Price SA, Vos RA, Gittleman JL, Purvis A. 2007. The delayed rise of present-day mammals. Nature. 446:507–512.

Bond J, Roberts E, Mochida GH, Hampshire DJ, Scott S, Askham JM, Springell K, Mahadevan M, Crow YJ, Markham AF, et al. 2002. ASPM is a major determinant of cerebral cortical size. Nat Genet. 32:316–320.

Borrell V. 2010. In vivo gene delivery to the postnatal ferret cerebral cortex by DNA electroporation. J Neurosci Methods. 186:186–195.

Borrell V, Del Rio JA, Alcantara S, Derer M, Martinez A, D'Arcangelo G, Nakajima K, Mikoshiba K, Derer P, Curran T, et al. 1999. Reelin regulates the development and synaptogenesis of the layer-specific entorhino-hippocampal connections. J Neurosci. 19:1345–1358.

Borrell V, Kaspar BK, Gage FH, Callaway EM. 2006. In vivo evidence for radial migration of neurons by long-distance somal translocation in the developing ferret visual cortex. Cereb Cortex. 16:1571–1583.

Boulder Committee. 1970. Embryonic vertebrate central nervous system: revised terminology. Anat Rec. 166:257–261.

Brazel CY, Romanko MJ, Rothstein RP, Levison SW. 2003. Roles of the mammalian subventricular zone in brain development. Prog Neurobiol. 69:49–69.

Bystron I, Blakemore C, Rakic P. 2008. Development of the human cerebral cortex: Boulder Committee revisited. Nat Rev Neurosci. 9:110–122.

Caviness VS, Jr.. 1975. Mechanical model of brain convolutional development. Science. 189:18–21.

Choi BH, Lapham LW. 1978. Radial glia in the human fetal cerebrum: a combined Golgi, immunofluorescent and electron microscopic study. Brain Res. 148:295–311.

deAzevedo LC, Fallet C, Moura-Neto V, Daumas-Duport C, Hedin-Pereira C, Lent R. 2003. Cortical radial glial cells in human fetuses: depth-correlated transformation into astrocytes. J Neurobiol. 55:288–298.

Dehay C, Giroud P, Berland M, Killackey H, Kennedy H. 1996a. Contribution of thalamic input to the specification of cytoarchitectonic cortical fields in the primate: effects of bilateral enucleation in the fetal monkey on the boundaries, dimensions, and gyrification of striate and extrastriate cortex. J Comp Neurol. 367:70–89.

Dehay C, Giroud P, Berland M, Killackey HP, Kennedy H. 1996b. Phenotypic characterisation of respecified visual cortex subsequent to prenatal enucleation in the monkey: development of acetylcholinesterase and cytochrome oxidase patterns. J Comp Neurol. 376:386–402.

Dehay C, Giroud P, Berland M, Smart I, Kennedy H. 1993. Modulation of the cell cycle contributes to the parcellation of the primate visual cortex. Nature. 366:464–466.

Dehay C, Kennedy H. 2007. Cell-cycle control and cortical development. Nat Rev Neurosci. 8:438–450.

Dehay C, Savatier P, Cortay V, Kennedy H. 2001. Cell-cycle kinetics of neocortical precursors are influenced by embryonic thalamic axons. J Neurosci. 21:201–214.

Engel AK, Muller CM. 1989. Postnatal development of vimentin-immunoreactive radial glial cells in the primary visual cortex of the cat. J Neurocytol. 18:437–450.

Englund C, Fink A, Lau C, Pham D, Daza RA, Bulfone A, Kowalczyk T, Hevner RF. 2005. Pax6, Tbr2, and Tbr1 are expressed sequentially by radial glia, intermediate progenitor cells, and postmitotic neurons in developing neocortex. J Neurosci. 25:247–251.

Fietz SA, Kelava I, Vogt J, Wilsch-Brauninger M, Stenzel D, Fish JL, Corbeil D, Riehn A, Distler W, Nitsch R, et al. 2010. OSVZ progenitors of human and ferret neocortex are epithelial-like and expand by integrin signaling. Nat Neurosci. 13:690–699.

Finlay BL, Darlington RB. 1995. Linked regularities in the development and evolution of mammalian brains. Science. 268:1578–1584.

Fish JL, Dehay C, Kennedy H, Huttner WB. 2008. Making bigger brains-the evolution of neural-progenitor-cell division. J Cell Sci. 121:2783–2793.

Gadisseux JF, Evrard P, Mission JP, Caviness VS, Jr.. 1992. Dynamic changes in the density of radial glial fibers of the developing murine cerebral wall: a quantitative immunohistological analysis. J Comp Neurol. 322:246–254.

Gong Q, Shipley MT. 1995. Evidence that pioneer olfactory axons regulate telencephalon cell cycle kinetics to induce the formation of the olfactory bulb. Neuron. 14:91–101.

Hansen DV, Lui JH, Parker PR, Kriegstein AR. 2010. Neurogenic radial glia in the outer subventricular zone of human neocortex. Nature. 464:554–561.

Herrmann K, Antonini A, Shatz CJ. 1994. Ultrastructural evidence for synaptic interactions between thalamocortical axons and subplate neurons. Eur J Neurosci. 6:1729–1742.

Hevner RF, Hodge RD, Daza RA, Englund C. 2006. Transcription factors in glutamatergic neurogenesis: conserved programs in neocortex, cerebellum, and adult hippocampus. Neurosci Res. 55:223–233.

Hilgetag CC, Barbas H. 2006. Role of mechanical factors in the morphology of the primate cerebral cortex. PLoS Comput Biol. 2:e22.

Hong SE, Shugart YY, Huang DT, Shahwan SA, Grant PE, Hourihane JO, Martin ND, Walsh CA. 2000. Autosomal recessive lissencephaly with cerebellar hypoplasia is associated with human RELN mutations. Nat Genet. 26:93–96.

Honig LS, Herrmann K, Shatz CJ. 1996. Developmental changes revealed by immunohistochemical markers in human cerebral cortex. Cereb Cortex. 6:794–806.

Howard B, Chen Y, Zecevic N. 2006. Cortical progenitor cells in the developing human telencephalon. Glia. 53:57–66.

Issa NP, Trachtenberg JT, Chapman B, Zahs KR, Stryker MP. 1999. The critical period for ocular dominance plasticity in the Ferret's visual cortex. J Neurosci. 19:6965–6978.

Downloaded from https://academic.oup.com/cercor/article/21/7/1674/339599 by guest on 23 April 2024

Jackson CA, Peduzzi JD, Hickey TL. 1989. Visual cortex development in the ferret. I. Genesis and migration of visual cortical neurons. J Neurosci. 9:1242–1253.
Johnson JK, Casagrande VA. 1993. Prenatal development of axon outgrowth and connectivity in the ferret visual system. Vis Neurosci. 10:117–130.
Kowalczyk T, Pontious A, Englund C, Daza RA, Bedogni F, Hodge R, Attardo A, Bell C, Huttner WB, Hevner RF. 2009. Intermediate neuronal progenitors (basal progenitors) produce pyramidal-projection neurons for all layers of cerebral cortex. Cereb Cortex. 19:2439–2450.
Kriegstein A, Noctor S, Martinez-Cerdeno V. 2006. Patterns of neural stem and progenitor cell division may underlie evolutionary cortical expansion. Nat Rev Neurosci. 7:883–890.
Krishna K, Nuernberger M, Weth F, Redies C. 2008. Layer-specific expression of multiple cadherins in the developing visual cortex (V1) of the ferret. Cereb Cortex. 19:388–401.
Letinic K, Zoncu R, Rakic P. 2002. Origin of GABAergic neurons in the human neocortex. Nature. 417:645–649.
Levitt P, Rakic P. 1980. Immunoperoxidase localization of glial fibrillary acidic protein in radial glial cells and astrocytes of the developing rhesus monkey brain. J Comp Neurol. 193:815–840.
Lohmann G, von Cramon DY, Colchester AC. 2007. Deep sulcal landmarks provide an organizing framework for human cortical folding. Cereb Cortex. 18:1415–1420.
Lohmann G, von Cramon DY, Steinmetz H. 1999. Sulcal variability of twins. Cereb Cortex. 9:754–763.
Lukaszewicz A, Savatier P, Cortay V, Giroud P, Huissoud C, Berland M, Kennedy H, Dehay C. 2005. G1 phase regulation, area-specific cell cycle control, and cytoarchitectonics in the primate cortex. Neuron. 47:353–364.
Manger PR, Kiper D, Masiello I, Murillo L, Tettoni L, Hunyadi Z, Innocenti GM. 2002. The representation of the visual field in three extrastriate areas of the ferret (Mustela putorius) and the relationship of retinotopy and field boundaries to callosal connectivity. Cereb Cortex. 12:423–437.
Marin O, Rubenstein JL. 2001. A long, remarkable journey: tangential migration in the telencephalon. Nat Rev Neurosci. 2:780–790.
Marin O, Rubenstein JL. 2003. Cell migration in the forebrain. Annu Rev Neurosci. 26:441–483.
Martinez-Cerdeno V, Noctor SC, Kriegstein AR. 2006. The role of intermediate progenitor cells in the evolutionary expansion of the cerebral cortex. Cereb Cortex. 16(Suppl 1):i152–i161.
McConnell SK, LeVay S. 1986. Anatomical organization of the visual system of the mink, Mustela vison. J Comp Neurol. 250:109–132.
Misson JP, Austin CP, Takahashi T, Cepko CL, Caviness VS, Jr. 1991. The alignment of migrating neural cells in relation to the murine neopallial radial glial fiber system. Cereb Cortex. 1:221–229.
Mo Z, Moore AR, Filipovic R, Ogawa Y, Kazuhiro I, Antic SD, Zecevic N. 2007. Human cortical neurons originate from radial glia and neuron-restricted progenitors. J Neurosci. 27:4132–4145.
Mo Z, Zecevic N. 2008. Is Pax6 critical for neurogenesis in the human fetal brain? Cereb Cortex. 18:1455–1465.
Mo Z, Zecevic N. 2009. Human fetal radial glia cells generate oligodendrocytes in vitro. Glia. 57:490–498.
Molyneaux BJ, Arlotta P, Menezes JR, Macklis JD. 2007. Neuronal subtype specification in the cerebral cortex. Nat Rev Neurosci. 8:427–437.
Neal J, Takahashi M, Silva M, Tiao G, Walsh CA, Sheen VL. 2007. Insights into the gyrification of developing ferret brain by magnetic resonance imaging. J Anat. 210:66–77.
Noctor SC, Flint AC, Weissman TA, Dammerman RS, Kriegstein AR. 2001. Neurons derived from radial glial cells establish radial units in neocortex. Nature. 409:714–720.
Noctor SC, Martinez-Cerdeno V, Ivic L, Kriegstein AR. 2004. Cortical neurons arise in symmetric and asymmetric division zones and migrate through specific phases. Nat Neurosci. 7:136–144.
Noctor SC, Scholnicoff NJ, Juliano SL. 1997. Histogenesis of ferret somatosensory cortex. J Comp Neurol. 387:179–193.
Noden DM, deLahunta A. 1985. The embryology of domestic animals. Developmental mechanisms and malformations. Baltimore (MD): Williams and Wilkins.
O'Leary DD, Borngasser D. 2006. Cortical ventricular zone progenitors and their progeny maintain spatial relationships and radial patterning during preplate development indicating an early protomap. Cereb Cortex. 16(Suppl 1):i46–i56.
Piao X, Hill RS, Bodell A, Chang BS, Basel-Vanagaite L, Straussberg R, Dobyns WB, Qasrawi B, Winter RM, Innes AM, et al. 2004. G protein-coupled receptor-dependent development of human frontal cortex. Science. 303:2033–2036.
Pillay P, Manger PR. 2007. Order-specific quantitative patterns of cortical gyrification. Eur J Neurosci. 25:2705–2712.
Polleux F, Dehay C, Kennedy H. 1997. The timetable of laminar neurogenesis contributes to the specification of cortical areas in mouse isocortex. J Comp Neurol. 385:95–116.
Polleux F, Dehay C, Moraillon B, Kennedy H. 1997. Regulation of neuroblast cell-cycle kinetics plays a crucial role in the generation of unique features of neocortical areas. J Neurosci. 17:7763–7783.
Rajimehr R, Tootell RB. 2009. Does retinotopy influence cortical folding in primate visual cortex? J Neurosci. 29:11149–11152.
Rakic P. 1972. Mode of cell migration to the superficial layers of fetal monkey neocortex. J Comp Neurol. 145:61–83.
Rakic P. 1988. Specification of cerebral cortical areas. Science. 241:170–176.
Rakic P. 1995a. A small step for the cell, a giant leap for mankind: a hypothesis of neocortical expansion during evolution. Trends Neurosci. 18:383–388.
Rakic P. 1995b. Radial versus tangential migration of neuronal clones in the developing cerebral cortex. Proc Natl Acad Sci U S A. 92:11323–11327.
Rakic P. 2003a. Developmental and evolutionary adaptations of cortical radial glia. Cereb Cortex. 13:541–549.
Rakic P. 2003b. Elusive radial glial cells: historical and evolutionary perspective. Glia. 43:19–32.
Rakic P. 2004. Neuroscience. Genetic control of cortical convolutions. Science. 303:1983–1984.
Rakic P. 2009. Evolution of the neocortex: a perspective from developmental biology. Nat Rev Neurosci. 10:724–735.
Ramon y Cajal S. 1891. Sur la Structure du Système Nerveux de l'Homme et des Vertébrés. Cellule. 7:125–178.
Rockland KS. 1985. Anatomical organization of primary visual cortex (area 17) in the ferret. J Comp Neurol. 241:225–236.
Ross ME, Walsh CA. 2001. Human brain malformations and their lessons for neuronal migration. Annu Rev Neurosci. 24:1041–1070.
Schmechel DE, Rakic P. 1979a. A Golgi study of radial glial cells in developing monkey telencephalon: morphogenesis and transformation into astrocytes. Anat Embryol (Berl). 156:115–152.
Schmechel DE, Rakic P. 1979b. Arrested proliferation of radial glial cells during midgestation in rhesus monkey. Nature. 277:303–305.
Sheen VL, Walsh CA. 2003. Developmental genetic malformations of the cerebral cortex. Curr Neurol Neurosci Rep. 3:433–441.
Sidman RL, Rakic P. 1973. Neuronal migration, with special reference to developing human brain: a review. Brain Res. 62:1–35.
Smart IH, Dehay C, Giroud P, Berland M, Kennedy H. 2002. Unique morphological features of the proliferative zones and postmitotic compartments of the neural epithelium giving rise to striate and extrastriate cortex in the monkey. Cereb Cortex. 12:37–53.
Smart IH, McSherry GM. 1986a. Gyrus formation in the cerebral cortex in the ferret. I. Description of the external changes. J Anat. 146:141–152.
Smart IH, McSherry GM. 1986b. Gyrus formation in the cerebral cortex of the ferret. II. Description of the internal histological changes. J Anat. 147:27–43.
Takahashi T, Misson JP, Caviness VS, Jr.. 1990. Glial process elongation and branching in the developing murine neocortex: a qualitative and quantitative immunohistochemical analysis. J Comp Neurol. 302:15–28.
Tekki-Kessaris N, Woodruff R, Hall AC, Gaffield W, Kimura S, Stiles CD, Rowitch DH, Richardson WD. 2001. Hedgehog-dependent oligodendrocyte lineage specification in the telencephalon. Development. 128:2545–2554.
Toro R, Burnod Y. 2005. A morphogenetic model for the development of cortical convolutions. Cereb Cortex. 15:1900–1913.

Downloaded from https://academic.oup.com/cercor/article/21/7/1674/339599 by guest on 23 April 2024

Van Essen DC. 1997. A tension-based theory of morphogenesis and compact wiring in the central nervous system. Nature. 385: 313–318.
van Praag H, Schinder AF, Christie BR, Toni N, Palmer TD, Gage FH. 2002. Functional neurogenesis in the adult hippocampus. Nature. 415:1030–1034.
Voigt T. 1989. Development of glial cells in the cerebral wall of ferrets: direct tracing of their transformation from radial glia into astrocytes. J Comp Neurol. 289:74–88.
Walsh CA. 1999. Genetic malformations of the human cerebral cortex. Neuron. 23:19–29.
Welker W. 1990. Why does cerebral cortex fissure and fold? A review of determinants of gyri and sulci. In: Peters A, Jones EG, editors. Cerebral cortex. New York: Plenum Press. p. 3–136.
Williams AL, Reese BE, Jeffery G. 2002. Role of retinal afferents in regulating growth and shape of the lateral geniculate nucleus. J Comp Neurol. 445:269–277.
Zecevic N. 2004. Specific characteristic of radial glia in the human fetal telencephalon. Glia. 48:27–35.
Zecevic N, Chen Y, Filipovic R. 2005. Contributions of cortical subventricular zone to the development of the human cerebral cortex. J Comp Neurol. 491:109–122.
Zhao C, Teng EM, Summers RG, Jr., Ming GL, Gage FH. 2006. Distinct morphological stages of dentate granule neuron maturation in the adult mouse hippocampus. J Neurosci. 26:3–11.
Zilles K, Armstrong E, Schleicher A, Kretschmann HJ. 1988. The human pattern of gyrification in the cerebral cortex. Anat Embryol (Berl). 179:173–179.

Downloaded from https://academic.oup.com/cercor/article/21/7/1674/339599 by guest on 23 April 2024